TECHNISCHE UNIVERSITÄT WIEN

VIENNA UNIVERSITY OF TECHNOLOGY

D I P L O M A R B E I T

"TOF-SIMS Investigations of Metal Impurities in Silicon"

ausgeführt am

Institut für Chemische Technologien und Analytik

der Technischen Universität Wien

unter der Anleitung von

Ao.Univ.Prof. Dipl.-Ing. Dr.techn. Herbert Hutter

durch

Lukas Widder

Otto Glöckel-Gasse 7

7210 Mattersburg

Wien, Mai 2008 Lukas Widder

Acknowledgements

Most important, I would like to thank Ao.Univ.Prof. Dipl.-Ing. Dr.techn. Herbert Hutter for the possibility to perform this diploma thesis in his research group. Furthermore, his guidance and his supply with knowledge and ideas for the right approach to present investigation tasks were quite essential. Also, Prof. Hutter has a unique ability to ensure a relaxed and mellow working atmosphere amongst the members of his group.

Very important for advances in my work in the last few months were also all the other members of our research group: Dipl.-Ing. Klaus Nowikow, Mag. Arno Schintlmeister, Dipl.-Ing. Johannes Schnöller, Dipl.-Ing. Stephan Puchner, Dipl.-Ing. Christoph Straif, and Nikolas Kornfeind.

Sincere thanks for all support in explaining technical details and the essential help in the use of the instrument. All the suggestions and discussions were extremely helpful and valuable.

Very special thanks go out to my colleague Dipl.-Ing. Markus 'Mol' Holzweber, most important for his support in bureaucratic questions during my studies, but also for inspiring discussions apart the university.

My very special thanks belong to my family and especially my parents for their enduring patience and caring support in all the years throughout my studies.

Last but not least, I want to thank all my colleagues and friends for their friendship during the last couple of years and their miscellaneous efforts to make this a pleasant time for me; rich of experiences and great memories.

Contents

1 Abstract

Microelectronic devices on semiconductor basis have become essential for every day life in recent years. Semiconductor industries are huge business branches that heavily compete over market superiority. Therefore, research and development in materials science has grown enormously. Silicon is the mostly used semiconductor material in microelectronic devices. It has been studied for many years and its properties are well known. As semiconductor devices become smaller and smaller, recent research has focused on impurities in active device regions that greatly decrease performance and lifetime.

In this work focus is on copper and sodium impurities in silicon. First, gettering effects in the silicon wafer bulk are investigated. Through ion implantation and annealing processes certain defects are produced in well controllable depths. Copper atoms diffusing through the wafer bulk gather at these lattice defect sites. This proximity gettering procedure is used to keep active device regions free of impurities.

Recent investigations of this problem have been done on the previous SIMS (secondary ion mass spectrometry) instrument, so comparability to the use of the new TOF-SIMS instrument was examined. Two different types of silicon, n-type silicon and highly boron doped silicon, respectively, are used to investigate copper gettering behaviour of oxygen, phosphorus, and silicon ion implanted wafer structures.

As a second subject of investigation surface diffusion of sodium into silicon was examined. Sodium is another impurity detrimental to semiconductor devices. It is almost ubiquitous and hardly controllable. During device manufacturing processes sodium consistently contaminates the silicon surface. In this paper, some preliminary studies of sodium diffusion after sodium containing molecules were applied onto the silicon wafer surface were conducted. Samples were annealed at various temperatures to investigate sodium diffusion barriers and behaviour.

All our measurements were carried out using the fairly new ION-TOF[5] instrument. Semiconductor industries work with highly pure silicon material, therefore already low concentrations of impurities can deteriorate the properties and characteristics of semiconductor devices. SIMS is an excellent analytic method to determine trace elements and impurities in metals and semiconductors due to its very low detection limits and the ability to measure depth profiles.

1.1 Kurzfassung

In dieser Arbeit wurde Diffusion von Kupfer und Natrium in Silizium untersucht. zuerst wurden Gettering Effekte in Silizium Wafern untersucht. Durch Ionenimplantation und thermische Behandlung werden bestimmte Defekt in Silizium generiert. An diesen Fehlstellen werden diffundierende Kupferatome gesammelt. Dieses Verfahren wird benutzt um in Halbleiterbauteilen aktive Regionen frei von Verunreinigungen zu halten.

Diese Messungen wurden durchgeführt um die Vergleichbarkeit des neuen TOF-SIMS Gerätes mit vorhergehenden Messungen zu überprüfen. Es wurden n-type und Bor-gedoptes Silizium untersucht, in das Sauerstoff, Phosphor oder Silizium Atome implantiert wurden.

Der zweite Teil beschäftigt sich mit der Oberflächendiffusion von Natrium in Silizium. In dieser Arbeit werden einleitende Versuche zu Diffusion von Natriumverunreinigungen in Silizium durchgeführt.

Alle Messungen wurden auf dem TOF-SIMS-Gerät der Arbeitsgruppe Prof. Herbert Hutter durchgeführt.

2 Introduction

2.1 General

Nowadays, semiconductor devices are used in numerous different technological fields and semiconductor industry is a steadily growing branch of high-tech manufacturing business. Therefore, much effort and financial resources for research and development have to be spent in order to gradually achieve improvement in their product quality. Material market's situations with progressively growing prices and end-consumer's demands require upcoming generations of semiconductor devices, such as microelectronic elements like transistors and diodes, to have improved performance and higher storage capacities than previous generations of alike components.

The steady increase of industrial productivity and enhanced performance of the products would not have been possible without equally impressive advance in materials science. Innovations have been achieved both in chemical compositions and in manufacturing processes. The industry today offers a huge number of high performance materials that are often application-tailored and meet highest analytical standards.

Most commonly used semiconductor devices are integrated circuits for microprocessor computer chips. These integrated circuits are electronic circuitries built on semiconductor substrates. For this purpose, usually wafers of single-crystal silicon are used. The production of silicon wafers for electronic devices itself has economic turnovers of about eight billion dollars a year. Integrated circuits are fabricated mostly including steps like film formation, photolithography, etching, impurity doping, and ion implantation. The yield in integrated circuits processing

is critically dependent on the effectiveness of the impurity gettering treatments after ion implantation.

Advanced device processing for increased performance, while at the same time essential downsizing of the elements is anticipated, requires efficient removal of metal impurities from active device regions, which in turn poses serious challenges for the development of novel and compatible gettering procedures. The technological importance of gettering arises from the fact that transition metals, such as Cu, create deep levels in the band gap [1], thus adversely affecting electrical characteristics, performance and reliability of the end-products.

High-energy ion implantation is being increasingly recognized as a promising method of achieving impurity gettering in silicon. In the so called 'proximity gettering' technique a gettering layer is formed in the bulk of the Si wafer near the active device area by means of ion implantation and annealing. The gettering layer collects unwanted metal impurities, thus reducing their concentration in the active device region.

Because of the demanded decreasing size of semiconductor devices and the importance to determine and understand the gettering of metal impurities in these complex systems the pressure on analytical methods also increases.

Secondary Ion Mass Spectrometry (SIMS) is an analytical method that has been in commercial use for over 30 years now. Its main advantages are the high detection sensitivity in ppm range for all elements, isotopic sensitivity, the possibility of depth profiling and the ability to record elemental images with a lateral resolution below 100 nm and three-dimensional images. These features have made SIMS an important tool in several fields of material science such as in steel industry, in the analysis of various thin film systems, and most important in semiconductor industry.

As this research for upgraded materials and improved device characteristics continues, these companies and research facilities tend to increasingly corporate with research groups at universities. Thus, large networks have been built between research centres of various universities and other research and development sections to advance in fundamental material science.

The analytical section of this diploma thesis will investigate gettering effects of copper ions in silicon wafers and thermal sodium surface diffusion into the silicon bulk, respectively. For the investigation of gettering abilities of defects created using high energy ion implantation, the research group of Dr. Kögler at the Forschungszentrum Rossendorf in Dresden provided samples for SIMS analysis. All necessary implantation and thermal annealing procedures were carried out by this research group.

The second part of the investigations, the thermal diffusion of sodium was done in cooperation with Infineon, one of the worldwide leading companies in semiconductor industry.

The following chapters will provide a general idea of the theoretical backgrounds and will introduce the analytical techniques and principals used for our investigations.

2.2 Silicon-Wafer Production

2.2.1 Czochralski - Silicon

The fast change in industries, science and society the most part is based on recent developments in microelectronic devices. These affect everyday life for everybody. As Moore's Law predicts, performance of electronic devices doubles in less than every two years. The basis of this tremendous growth was single crystals of silicon with very high purity and near perfect crystal structure. Around 95% of today's monocrystalline silicon productions are produced using the Czochralski-technique; accidentally discovered by polish Jan Czochralski in 1916 as he was investigating crystal growth of metal melts [2].

For the production of semiconductor devices the polycrystalline silicon is converted into the single crystal state. Today, large silicon ingots with diameters of 300 mm are used for silicon wafer production. Research and development of semiconductor industries these days are even working on application of single crystals with diameters of 450 mm.

The Czochralski-method uses a large fused crucible made of quartz. In this crucible the electron grade high purity silicon is then melted down. In this stage also dopant impurity atoms for production of n-type or p-type silicon can be added to the molten intrinsic silicon to influence the electrical conductivity. For crystal growth a small silicon single crystal is mounted on a long rotating metal shaft to be dipped into the melt inert gas atmosphere. This seed crystal of about 0.5 in diameter cm will determine the orientation of the final silicon single crystal of the ingot.

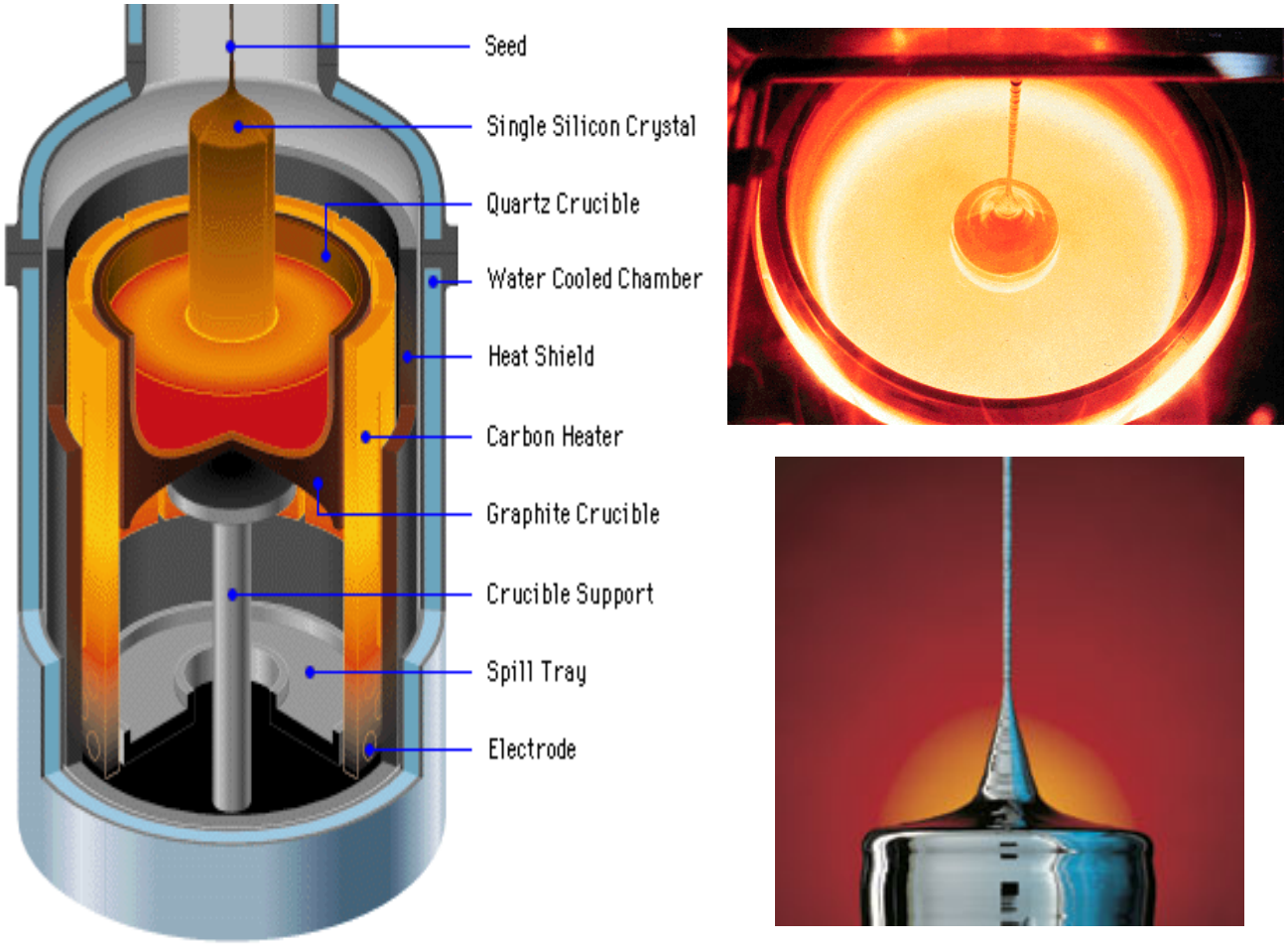

Figure 1: Czochralski crystal growth method

As the seed crystal is pulled out of the molten silicon it is also slowly rotated at the same time. The melt is pulled away from the molten silicon due to surface tension between the seed crystal and the melt. On the expanding surface area the melt will solidify as it is cooling down. By precisely controlling the temperature gradients, rate of pulling and speed of rotation, it is possible to extract a large, single-crystal, cylindrical ingot from the melt. During the crystal growth some amounts of the walls of the crucible made of quartz will dissolve into the melt and cause oxygen impurities to be contained in the final silicon single crystal.

2.2.2 Silicon Wafer Production

For the production of a flat and clean silicon wafer as carrier material for integrated circuits final processing steps are necessary. Semiconductor devices are fabricated on mirror polished silicon wafers and therefore, mirror polished and damage-free silicon surfaces are fabricated.

The first step is to produce silicon slices of the ground ingot. This defines critical mechanical characteristics of the silicon such as thickness, warp, bow, and tarp. For slicing commonly an inner diameter circular saw with a diamond coated blade or a multiple wire saw made of stainless steel wires are used.

To remove mechanical surface damage left by slicing, the resulting silicon slices are then chemically etched by an acidic solution. Mostly used are mixtures of nitric acid and hydrofluoric acid solutions using common modifiers such as glacial acetic acid. In this two-step process HNO_3 will oxidize the surface to SiO_2 which is removed by HF. Subsequent treatment with acetic acid will produce a shining surface.

In a next step the edges of the silicon wafers are rounded to reduce mechanical defects that could act as dislocation and defect source during annealing. The silicon wafers are then mechanically lapped to remove any remaining damage caused by previous production steps and to produce absolute flatness of the surface. Therefore, an abrasive solution of micro-sized alumina or silicon carbide particles in water is used.

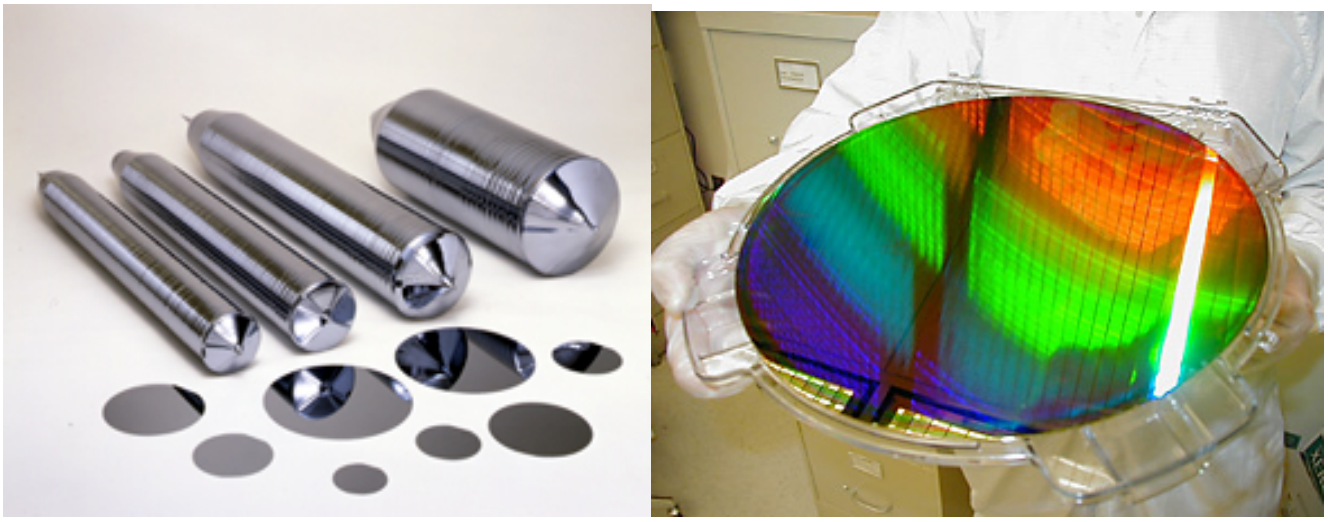

Figure 2: CZ-Si processed into silicon wafers

Finally, the wafer is polished by chemical-mechanical polishing. For this method a synthetic leather polishing pad and an alkaline colloidal solution of silica particles are used. This process step is used to produce an optical reflective mirror-finished surface to support optical photolithography, which is needed for most semiconductor applications. However, this procedure slightly decreases the wafer surface flatness achieved by lapping [3]. Final chemical cleaning steps are added to reduce wafer surface contaminations that can greatly reduce electronic device performance.

2.2.3 Production of Integrated Circuits

These silicon monocrystalline wafers are the main substrate used for integrated circuits on semiconductors. They are produced by means of a layer process using photolithography to define individual circuit elements. In this process UV-light is used to transfer microscopic patterns from a photo mask onto a light-sensitive photoresist on the silicon wafer.

The silicon wafer is spin coated with the photoresist polymer, which reacts to treatment with UV-radiation. The polymer film is then exposed to intense radiation in a certain pattern through transparent areas of the photomask. This radiation chemically changes the photoresist and solubility for patterned regions differs from non-radiated areas. In the positive photoresist method UV-exposed areas are removed by the 'developer' solutions like tetramethylammonium hydroxide (TMAH).

In the following etching step the uppermost layers of the substrate that are not protected by the photoresist anymore are removed by the use of chemicals.

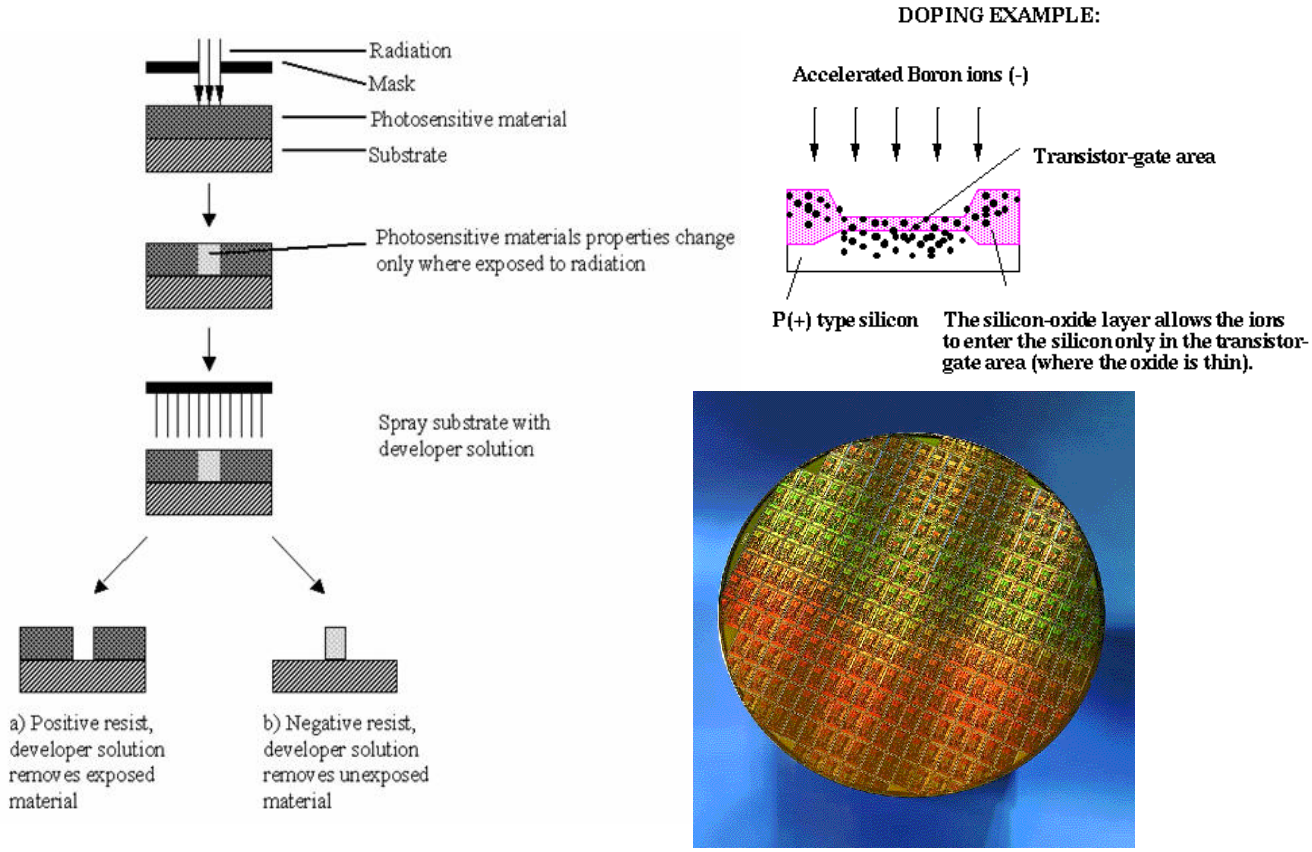

Figure 3: Photolithography procedure; dopant introduction using ion implantation method; processed wafer containing microprocessor devices

For the production of certain circuit elements such selected areas defined by photolithography are further doped by impurity atoms to modify electrical properties and conducting abilities. Therefore, specific impurities are intentionally introduced by means of such processes like diffusion or ion implantation [4] into areas not protected by a resist. The remaining photoresist on the silicon substrate is then removed by chemical resist strippers. Additionally, annealing steps are applied to relax damages in the crystal lattice structure.

To form an active circuit element a single wafer may have to undergo many successive process steps to achieve the complex layers of conductor, semiconductor, and insulating material needed to produce the desired circuitry. Many modern chips have more than ten levels produced in many hundreds of sequenced processing steps.

2.3 Impurity Diffusion in Silicon

2.3.1 Fick's Law of Diffusion

One of the main approaches to diffusion is to treat diffusing substances as continuous media and to ignore the atomistic nature of the diffusion process. To quantify the distribution of atoms, the concentration is introduced as number of atoms per unit volume. Typically, in a system consisting of several species, only one of them is chosen for calculations. The simultaneous rearrangement of silicon atoms is of minor importance compared to the redistribution of an impurity in silicon.

The diffusion current *J* of the species under consideration can be related to the gradient of their concentration C by Fick's first law of diffusion, which represents a macroscopic definition for the diffusion coefficient D:

$$J = -D \cdot gradC$$

J	diffusion flux
D	diffusion coefficient
C	concentration

The negative sign indicates that the diffusion occurs towards the direction of decreasing concentration. The product of concentration and diffusion coefficient is known as transport capacity. In general, diffusion coefficients and transport coefficients will depend on temperature and may depend also on the concentrations of all impurities in the system, on the concentrations of charge carriers, crystal defects, and on pressure. The temperature dependence of diffusion coefficients determined from experiments is found to obey an Arrhenius relation:

$$D = D_0 \cdot \exp\left(-\frac{E_A}{k \cdot T}\right)$$

D_0	diffusion prefactor
E_A	activation energy

For non steady diffusion and continually changing diffusion over time Fick's second law of diffusion is used:

$$\frac{\partial C}{\partial t} = D \cdot \nabla^2 C$$

It provides a relation between chronological and regional differences of concentration in unsteady diffusions and can also describe diffusion in solids. Solutions to this equation depend strongly on initial and boundary values.

2.3.2 Basic Diffusion Mechanisms

In a perfect crystal every lattice atom oscillates around its permanent lattice position but can not leave this site. For diffusion in a crystalline solid a prerequisit condition is the presence of defects in the lattice. The change of locations of atoms in the crystal as requirement for transport of matter can only be achieved through defects in the crystal structure. For diffusion in solids different mechanisms are possible.

Influences of the concentrations of vacancies and self-interstitials reflect the actual atomistic mechanism of diffusion. Impurity diffusion and their interaction with intrinsic point defects needs to be discussed in more detail.

Interstitial Impurities

Because of the very open nature of the silicon crystal many atoms dissolve on interstitial sites between the lattice atoms and diffuse in such manner. These include most alkali, like sodium, and heavy metals like copper and iron, but also hydrogen and oxygen. Such interstitial sites show low concentrations of atoms, therefore all neighbouring interstitial sites can, in general, be considered vacant. As a consequence, these atoms perform a random walk, characterized by a diffusion coefficient, which is a function of temperature only; magnitudes larger than self-diffusion and group III and V dopant's coefficients.

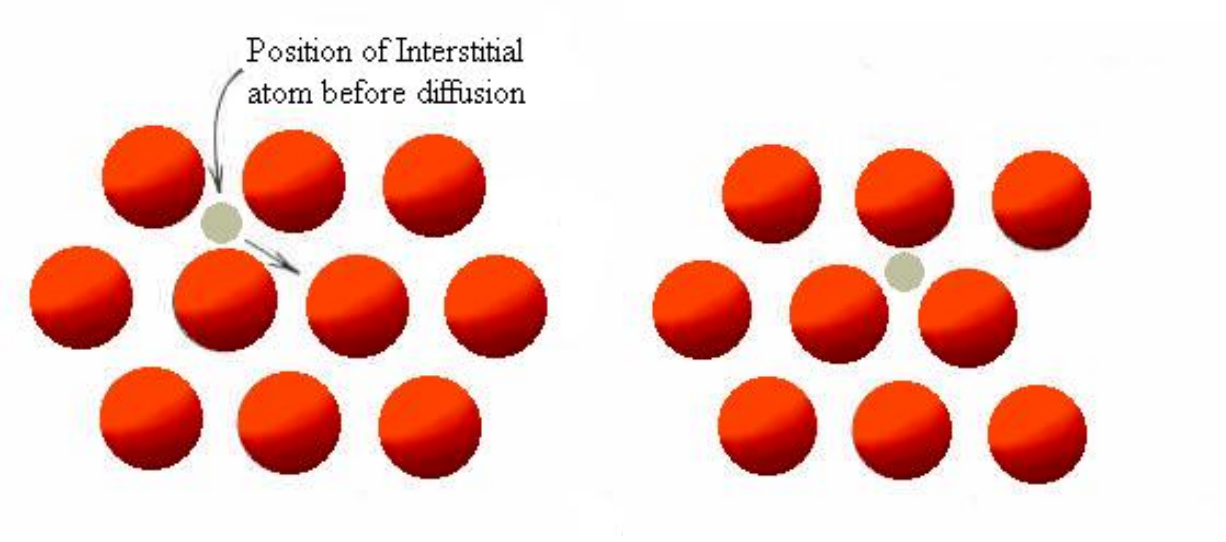

Figure 4: Interstitial diffusion mechanism

There is also an indirect interchange mechanism possible. In this model, first a lattice atom is leaving its substitutional site, then one of the neighbouring atoms is moving into the vacancy left behind, while the first atom moves from the interstitial position onto the vacancy left behind.

At exceeding impurity concentrations on interstitial sites impurities may form precipitates. Because of the high diffusivity precipitation can occur even at moderate temperatures. Forming in active device areas, such precipitates can reduce drastically device performance and yield. It is therefore desirable to getter detrimental interstitial diffusers in areas where they do not cause harm.

Substitutional Diffusion

In semiconductor industry atoms of the groups III and V of the periodic table are most important as dopants in silicon. They reside predominantly in ionized form on substitutional sites and have comparatively low diffusion coefficients.

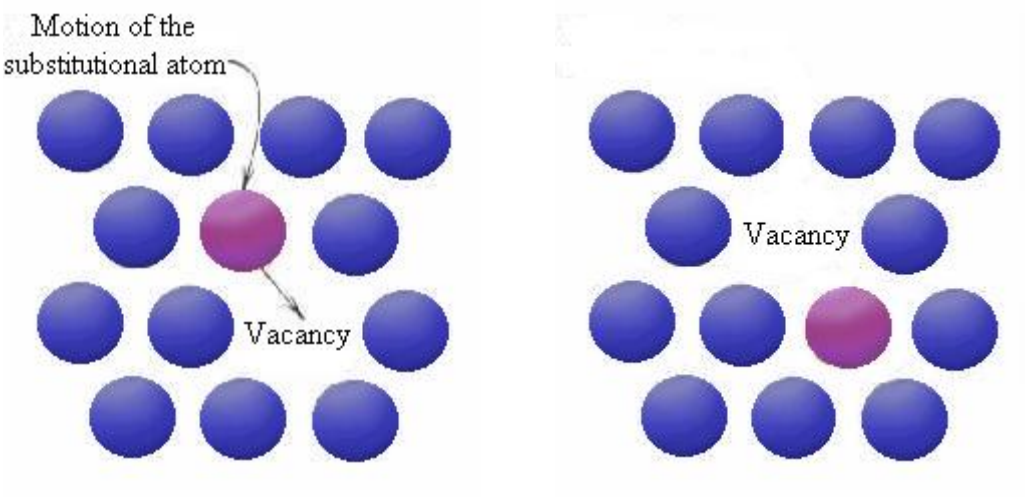

Figure 5: Substitunial impurity diffusion

In general, the diffusion of substitutional atoms is assumed to proceed with the help of intrinsic point defects. One possible mechanism is that substitutional atoms exchange positions with adjacent vacancies

evoking a net flux of diffusing atoms. Consequently substitutional diffusion is only possible if the lattice has a number of vacancies, or empty lattice sites, scattered throughout the crystal, so that there are places into which the impurity can move.

Moving interstitially requires energy to get over the potential barrier of the regions between the lattice sites. Energy is also required to form the vacancies for substitutional diffusion. Thus, for either form of diffusion, the diffusion coefficient is a function of temperature.

Impurity-Point-Defect Pairs

The dominant mechanism considered for the diffusion of substitutional impurities includes the formation of impurity-vacancy pairs. This impurity-vacancy binding leads to a series of migration steps of these pairs without dissociation.

The two different types of point defects, the vacancy and the self-interstitial, have different roles in diffusion. Is an unassociated vacancy moving to the nearest-neighbour site of an impurity atom, the impurity atom is able to exchange its position with the vacancy, if it has acquired enough kinetic energy. There might be also the chance that the impurity atoms moves back to its original site, exchanging positions with the vacancy. This situation would cause no diffusion at all.

However, if there exists a concentration gradient, impurity atoms in the region of higher concentration are more likely to capture the vacancy site than impurity atoms in the lower-concentration side. This leads to a net diffusion flux of the impurity atoms. Consequently, this flux is proportional to the concentration of the vacancies, and also the concentration gradient of the impurity atoms. This type of diffusion,

conventionally referred to as the vacancy mechanism, involves the movement of two species.

Self-interstitials, on the other hand, assist the diffusion of the impurity atom by kicking out the contaminant from its substitutional site, thus creating a more mobile species at an interstitial site. This is the so called kick out mechanism. There are two possible ways for the interstitial impurity to move. First, it can be restored back to the substitutional site by colliding with a neighbouring lattice atom or second, by being trapped by a vacancy site (Frank-Turnbull mechanism).

2.4 Gettering

Gettering is defined as the process of removing device degrading impurities from the active circuit regions of a wafer. It can be performed during crystal growth or in subsequent wafer fabrication steps. For integrated circuit manufacturing it is a very important measure for enhancing the yield.

In recent years the use of ion implantation induced defects as efficient gettering sites for metal impurities in silicon has generated much interest. To precisely introduce dopants into silicon one standard procedure in electronic device technology is ion implantation.

During implantation of the ions damages of the crystalline structure of the semiconductor material are generated. After an annealing step residual damages act as effective gettering centres of impurities, such as transition metals in silicon. Through high-energy ion implantation the impurity gettering can be used to collect unwanted metal

contaminations in gettering layers close to the active device region and so reduce their concentration in the device areas. This is referred to as "proximity gettering."

After ion implantation and annealing, one gettering layer forms in a layer around the projected ion range, R_P. This gettering band corresponds to a layer of secondary defects, such as dislocation loops and interstitials and voids, which form during annealing steps through the excess of self-interstitials, also observable by cross-section transmission electron microscopy.

Another gettering layer is formed by ion implantation not only around the main projected range R_P, but also in another distinct depth region between surface and R_P, roughly centered at half of this range, $R_P/2$ [5,6,7,8], where excess vacancies cluster to empty cavities.

Along the trajectory of an implanted ion silicon atoms are displaced and relocated. Each atom displacement results in one self-interstitial silicon atom and one vacancy, which are referred to as a Frenkel-pair. During this process of ion implantation the forward momentum of the impinging ions generates excess vacancies in the region before R_P and excess interstitials at R_P. The spatial separation of the radiation-induced Frenkel-pair's vacancies and interstitials on average leads to a vacancy-rich region at $R_P/2$ whereas an excess of self-interstitial silicon atoms is present in the R_P region.

Additionally, a third gettering layer can be found in a region even deeper than the projected ion range. This occurrence is referred to as the *trans*-R_P-effect and to this point it is only observed if dopants like P^+ or As^+ ions are implanted [9, 10, 11, 12]. Formation of these *trans*-R_P defects proceeds during the annealing treatment by point defect and dopant diffusion and probably consists of interstitial clusters.

2.5 Topics of Investigation

Traditionally, semiconductor industry is based on silicon as the raw material. The knowledge and information about silicon materials and their electrical properties and behaviour is enormous. Improvements in this field of research to enhance device quality and material characteristics are an essential ambition for the future.

One ambition is to efficiently reduce impurity concentrations during production and processing steps. In advanced microelectronics device fabrication thorough removal of metal impurities from active device regions is required. These metal impurities are detrimental to these active device regions and strongly degrade properties of silicon semiconductor devices. They can act as electron donors and have high mobility. Therefore, if active regions of semiconductor devices are heated this can lead to accumulation and high concentrations of impurities in these areas. Contaminations of other metal atoms can strongly influence electrical properties of semiconductor devices by introducing levels in the forbidden band gap, which can act as compensators and charge carrier traps.

2.5.1 Cu-Gettering in Silicon

For many years different contaminants in silicon like iron, nickel or aluminium have been investigated. In addition, copper (Cu) and other transition metals are known to deteriorate the device characteristics if they are present in too high concentrations in active device regions. Recently, the attention has shifted towards copper since this is a widespread contaminant in silicon. Therefore, special interest has risen regarding the Cu redistribution and trapping by device structures and

crystal damage during thermal processing. Different gettering methods were being investigated.

One of the most promising gettering methods relies on high energy implantation and is known as ‘proximity gettering.’ Therein, buried layers of mega electron volt ion implantation induced defects to getter metal impurities are produced. Thus, the mechanisms and nature of the gettering centres have to be investigated. In recent studies different gettering sites depending on implantation energy and ion sort in various depths of the implanted silicon wafers have occurred.

In this paper, the possibilities of Cu gettering measurements in silicon with the new ION-TOF^5 instrument and the comparability to previous data acquisitions on equally composed samples are studied. Former investigations have been carried out with an upgraded Cameca IMS 3f instrument. For this paper, implants of 200 and 450 keV and different implant ions are investigated.

2.5.2 Na - Diffusion into Silicon

Another omnipresent contaminant in silicon is sodium (Na). It is also one of the main impurities that current research is eager to avoid in active device regions. As Na is present in most surroundings the majority of device surfaces are contaminated.

This paper will introduce preliminary studies on the surface diffusion of Na. Depth profiling was performed for investigations of two different sodium involving molecules over a range of different temperatures to find a proper contamination source for diffusion investigations.

Eventually, the aim of further investigations is to determine origins of sodium including molecules and which surface contaminants are most likely to release Na for diffusion into the bulk. Mechanisms forming the basis for sodium diffusion are of considerable interest as well. More investigations in the future are supposed to provide activation energies and diffusion coefficients for Na diffusion in silicon.

3 The TOF-SIMS method

3.1 General Information

Secondary Ion Mass Spectrometry is a surface analysis method based on sputtering processes used to characterize the surface and sub-surface regions of materials. In materials science it is used in many different fields of interest due to its vast range of application possibilities.

SIMS plays a very important and powerful role in analysis of trace elements in numerous different matters such as semiconductors, thin film coatings and various high performance materials. With SIMS it is possible to detect all elements including hydrogen within a typical detection sensitivity of parts per million (ppm) for most elements and parts per billion (ppb) for favourable elements and it is also able to distinguish between various isotopes of one element.

The main advantages of the SIMS measurement technique are its already mentioned high sensitivity, a large dynamic range, and the possibility of measuring depth profiles, all with excellent lateral and depth resolution in the low nano-meter range. It is also proficient to record direct surface images and detect 3D-distributions of the different ion species. Due to these advantages the uses of SIMS spread over fields like metallurgy, geology, glass and ceramics compositions, biosensors and cell biology, medicine and drug development in pharmacy. But the main field of application remains definitely the semiconductor industry where SIMS is used for process and production monitoring and optimization procedures.

The basic principles of Secondary Ion Mass Spectrometry were first presented and introduced by the pioneers R. F. K. Herzog and F. P. Viehböck in the year 1949 [13]. From this point on, many improvements and adaptations leading to enormous progress in measuring capabilities and quality have been made.

3.2 Fundamentals of SIMS

SIMS is based on the principle that it effectively employs mass spectrometry on the charged atoms and molecules which are emitted when a solid sample surface is sputtered, i.e. bombarded by energetic primary particles.

Typical ions for particle bombardment are O_2^+, Cs^+, Ar^+ Ga^+ or Bi^+ in an energy range 0.5 to 25 keV. The focused, pulsed incident primary ion beam distributes its energy in the sample surface through processes like backscattering, recoil implantation and collision cascades. These actions are determined by mass, energy, angle of incidence of the impinging ions, the current density of the primary beam and the atomic mass and surface binding energy of the sample atoms. Due to the fact that this energy transfer normally takes place in the most upper atomic layers particles of the first to third atomic layers are ejected as sputtering yield.

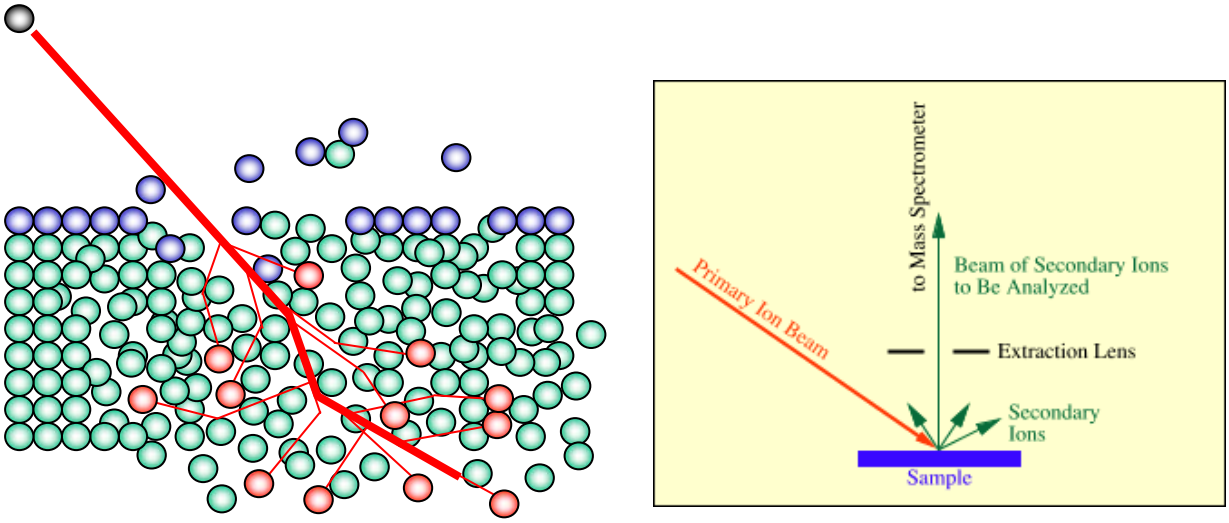

Figure 6: Principles of SIMS measurements

The amount of ejected charged particles per incident primary ion, which is the definition of the SIMS ionization efficiency, depends on the physical properties and normally varies between 0.1 to 15 atoms per primary ion. However, most particles that are released from the sample surface are uncharged. Only approximately 0.001 to 1% of the particles are ionized and can be extracted via the extractor field and enter the mass analyzer of the mass spectrometer.

Besides single charged particles, also multiple charged atom clusters and molecular fragments can be generated. Furthermore, in addition to particles emerging from the actual sample surface also resputtered primary ions, as well as neutral particles, along with electrons and photons are included in the sample leaving beam. Primary ions mix with sample atoms due to implantation of several nm into the sample.

Basically TOF-SIMS is based upon the principle, that particles with equal kinetic energy E_{kin} and different mass m require different time periods to glide through a certain distance of a field free drift zone with length L. Therefore it is necessary to determine the time-of-flight t very precisely. This is overcome by the use of short pulses of primary ions, which allows exact determination of the starting times. The secondary ions emitted from the surface are all accelerated into an electrical field with potential difference E_{pot}. When leaving the field the particles should have an equal constant kinetic energy E_{kin}.

$$E_{pot} = q \cdot U_0 = \frac{m \cdot v^2}{2} = \frac{1}{2} m \left(\frac{L}{t} \right)^2 = E_{kin}$$

$E_{pot,kin}$	potential and kinetic energy, respectively
U_0	acceleration voltage
q	charge of an ion
v	velocity of the particle
L	length of the mass analyzer
m	mass of each ion
t	time of flight

Of each single ion pulse ions split during the drift, as their velocity depends on their mass. The generated secondary ions with the charge q and the mass m the time of flight are measured through their mass to charge ratio.

$$t = \frac{s}{v} = L \cdot \sqrt{\frac{m}{2 q U_0}}$$

The mass resolution R of the TOF-SIMS mass analyzer is defined by following equation:

$$R = \frac{m}{\Delta m} = \frac{t}{2 \cdot \Delta t} = \frac{t}{2 \cdot \sqrt{\Delta t^2_{prim} + \Delta t^2_{drift} + \Delta t^2_{analyzer}}}$$

Δt_{prim} primary pulse width

Δt_{drift} energy distribution leading to a flight time difference for different ions with the same mass

$\Delta t_{analyzer}$ precision of the registration system

Generation of secondary ions leads to a width of the energy distribution of some eV [18]. Consequently, the flight time difference is primarily defining the mass resolution. For energy focussing a reflectron type of detector is used in the mass analyzer which results in a higher mass resolution.

3.3 Analytical Characteristics

3.3.1 Advantages of SIMS

Low Detection Limits:

The detection limit of SIMS ranges from parts per million atoms for most elements, including insensitive elements, to low parts per billion atoms for favourable and more sensitive elements. Sensitivity of elements can also be improved by enhancing the ionization probability using primary ions, which have high electronegativity (Oxygen), enhancing ionization probability for electropositive elements as well as low electronegativity (Caesium) for highly electronegative elements.

Possibility to Detect all Elements and Isotope Specificity:

With secondary ion mass spectrometry it is generally possible to detect all elements at the same time and also characterize and distinguish specific isotopes of one element. The limits depend on the mass resolution Δm/m, which for our Ion-TOF^5 equipment is above 10 000 and for heavy molecules even a mass in ranges up to 10 000 atomic units can be detected.

Surface Sensitivity:

If the sample is bombarded with the primary ions these ions will be implanted in a depth of about 10nm and also the surface structure of the sample will be altered. This enhances further segregation and

diffusion. In addition, atoms of the sample can be pushed forward deeper into the sample by incoming primary ions, which can cause a broadening of the signals.

The interaction of primary ions and target surface atoms usually is described by the collision cascade model. Therein, a fast primary ion passes its energy to sample atoms through a series of binary collisions. These energized target atoms can collide with more target atoms and recoil back through the sample surface, where they make up the sputtered matter and secondary ions. Thus, these incidents can reduce the depth resolution of secondary ion mass spectrometry.

High Depth Resolution:

Generally depth resolution is depending on the energy and the impact angle of the primary ions, and the mass and atomic number of both the primary ions and the target atoms in the sample. Besides instrumental and sample-related factors, the depth resolution of SIMS depends on the nature of the ion-solid interactions. Most important processes are atomic mixing, recoil implantation, radiation-induced diffusion and chemically driven segregation. Among these, atomic mixing often plays a dominant role. In order to get high depth resolution this effect should be minimized. It can thus be reduced by primary beam energy decrease, due to a decreased penetration depth of the primary ions and also a grazing incidence, but only at the expense of sputtering rate and crater shape. Hence, the better the depth resolution the worse the sputter yield.

Insulators Are Analysable as well:

Insulators and also sequences of conducting and insulating layers are measurable. However, on insulating target samples positive electrostatic charges appear during analysis, resulting from implantation of primary ions and subsequent emission of secondary electrons. These charging effects may have an effect on ionization probabilities and may cause electrical fields affecting the channelling of the secondary ions. Consequently, quantification and ion imaging can be constricted. Electron flood guns may be applied in order to reduce and balance charging effects.

3.3.2 Disadvantages of SIMS

Difficulties in Quantification:

Quantification in SIMS is a difficult and challenging task. There are versatile problems. First, there is the need of standards and Relative Sensitivity Factors (RSF) for quantification. Also, the ionization probability of a certain element not only depends on the element itself but is also affected by the chemical surrounding and matrix effects. Furthermore, instrumental parameters like primary beam size or vacuum can vary and in order to obtain proper quantitative statements standards need to have equal composition as the sample, so numerous standards are required. This can lead to a decrease in accuracy of quantification.

High Vacuum Conditions Needed:

Only samples that withstand high vacuum conditions are measurable because a high vacuum of about 10^{-8} mbar is applied to reduce impacts of remaining atmospheric gas molecules or other particles that would cover the surface. Moreover, high vacuum conditions are demanded to maximize the mean free path so collisions between ions and particles can be avoided.

Small Samples and a Destructive Method:

The samples must fit into the relatively small sample chamber, which drastically limits sample size. SIMS method is a destructive analysis and therefore measurements can not be repeated on the same sample volume. Obviously, samples that are of immense pecuniary or archaeological and cultural value therefore should not be damaged during investigations. This kind of samples are not appropriate for SIMS measurements and other analysis methods are indicated.

Interpretation of Mass Spectra is Demanding:

In mass spectra of solids many different peaks have to be assigned to certain ions and molecules. Secondary ion yields are often matrix dependent and vary by over six orders of magnitude throughout the periodic table. Detection limits and resolution depend on the sample material as well and therefore spectra can become extremely complicated. Atmospheric gas residues and organic contaminations on surfaces and all fractions of their large molecules contribute to the spectrum. Therefore numerous different ion peaks of atomic ions and all the isotopes of an element, molecule fractions and cluster ions, possibly

also multiply charged, get detected and appear in the spectrum, which can immediately add up to a very confusing accumulation of peaks. Additionally, masses which are concentrated close together will interfere and peaks will not be sharp but have shoulders and broaden.

3.4 TOF-SIMS instrumentation

3.4.1 Analysis Gun

All experiments presented in this work have been carried out on an instrument of the ION-TOF^5 type. The ION-TOF^5 is equipped with one ion gun for analysis, due to the time-of-flight principle it has to generate short, intense pulses for high mass resolution and one low energy ion gun for sputtering and sample erosion.

The standard analysis gun used in the ION-TOF^5 instrument is a Bi-cluster gun. It is a 25 keV liquid metal ion gun (LMIG) [19], which provides the opportunities to analyze samples not only with ionized Bi_1 atoms but also with clusters of Bi atoms (Bi_3^+, Bi_3^{++}, Bi_5^+). Separation to evade mass interference of the different Bi-clusters is done with the help of a pre-chopper.

The analysis gun can be operated in various modes which are optimized for certain tasks and describe compromises between maximum efficiency of categories such as pulse width for good mass resolution, beam size for lateral resolution and beam current for data acquisition rates.

	HIGH CURRENT MODE (2 crossovers)	BURST ALIGNMENT MODE (one crossover)	COLLIMATED MODE (no crossover)	LOW CURRENT SE MODE (2 crossovers)
static mode (DC)	beam alignment, SE images (1-4 µm @ 12...25 nA)	beam alignment, SE images (250 nm @ 1 nA)	beam alignment, SE images (100 nm @ 50 pA)	SE images (60 nm @ 10 pA)
"long" pulses (20 to 100 ns)	surface spectroscopy and mass resolved imaging with unit mass resolution and moderate lateral resolution (1 - 4 µm with DC equivalent current)	surface spectroscopy and mass resolved imaging with unit mass resolution at high lateral resolution (250 nm with DC equivalent current)	surface spectroscopy and mass resolved imaging with unit mass resolution at ultrahigh lateral resolution (100 nm with DC equivalent current)	
short pulses (approx. 1.5 ns) or burst of short pulses (6 ions/pulse)		surface spectroscopy and mass resolved imaging with high mass resolution (300 nm with 6 ions/pulse)		
bunched mode (< 800 ps)	High current bunched mode surface spectroscopy, depth profiling, and mass resolved imaging with ultrahigh mass resolution at moderate lateral resolution (2...10 µm @ 0.5...3 pA)			

Table 1: Operation modes of the ION-TOF^5 instrument [20]

For this work only the *high current bunched mode* was used. This mode is usually applied for depth profiling; it increases the current density and as a result generation of secondary ions is increased. High current bunched mode is mostly applied for surface spectroscopy, depth profiling, and mass resolved imaging with particularly high mass resolution at moderate lateral resolution.

3.4.2 Sputter Gun

As a sputter ion gun for sample erosion the ION-TOF^5 instrument provides a dual source ion column (DSC). This is a low energy ion gun with an energy range of 200 eV up to 2 keV, equipped with two different ion sources. These sources are a thermal ionization caesium source for profiling secondary ions of electronegative elements in negative SIMS mode and an electron impact gas ion source with oxygen for reactive gas operations to profile electropositive elements in positive SIMS mode.

In the electron impact ion source (EI source) the standard gas used is oxygen as for this allows metal-oxygen bonds to be formed in oxygen rich zones after O_2 ion bombardment or chemisorption. Here, the *broken bond model* for ionization as a consequence from the division of an ionic or covalent bond applies.

An electropositive surface atom is ionized by breaking the surface bonds to other atoms leaving an electron behind. The oxygen becomes negatively charged because its high electron affinity favours electron capture and positive charging is inhibited by its high ionization potential. Thus, the metal atom departs from the surface as positively charged ion. This way the ionization probability for electropositive elements can be increased to up to three times greater yield [17].

The thermal ionization caesium source (Cs^+ source) is used for enhancing the ionization probability for electronegative elements increasing the amount of negative secondary ions produced.

Here, the *electron tunnelling model* is valid for submonolayers of Cs deriving from a Cs sputter ion gun performing a depth profile. Due to the dependence of the ionization proability on the work function of the

surface, lowering work functions as much as possible enables charge transfer to the sputtered atoms. This way, more secondary electrons are tunnelled over the surface potential barrier. This increased availability of electrons leads to an increased negative ion formation [14, 15]. Another model is valid for clusters of ions of surface atoms with Cs atoms caused by the sputter beam. It suggests the recombination of Cs^+ ions with neutrals M from the matrix to form MCs^+ or MCs_2^+ clusters of ionic character. These molecules induce surface dipoles, reducing the work function of the sample [16].

3.4.3 The ION-TOF^5 Mass Analyzer

The time-of-flight SIMS instrument basically records a mass spectrum of secondary ions generated by an incoming ion beam. In the time-of-flight mass spectrometer the mass dependent time for ions to travel from the surface, being the ion source, to the detector is measured. Since this requires precise definition of the starting time ions are formed by a pulsed ionization method

The primary ions are applied by the use of a pulsed beam and each pulse of primary ions generates data points of which each is an entire mass spectrum where all generated secondary ions are contained, albeit these single pulse spectra are of very low intensity. During the dead time in between subsequent pulses sputter ions to erode the surface or charge decompensation can be applied. Of each single ion pulse the generated secondary ions with the charge q and the mass m the time of flight is measured through their mass to charge ratio.

The TOF-SIMS^5 instrument uses a reflectron type mass analyzer. As the secondary ions leave the surface the generated ion packet does not

have same kinetic energies and starting times due to energy distribution and other experimental factors such as delayed ion formation. So, the reflectron is supposed to compensate for these differences and optimize the mass resolution. The reflectron increases resolution by simply extending the path length.

The secondary ions have to pass through an extractor electrode into the mass analyzer. Before they hit the detector, the ions are deflected by the reflectron, which is an ion-optical deflection unit of the analyzer that acts in a similar way as a photo-optical mirror. The single stage electrostatic mirror is combined with two linear drift regions.

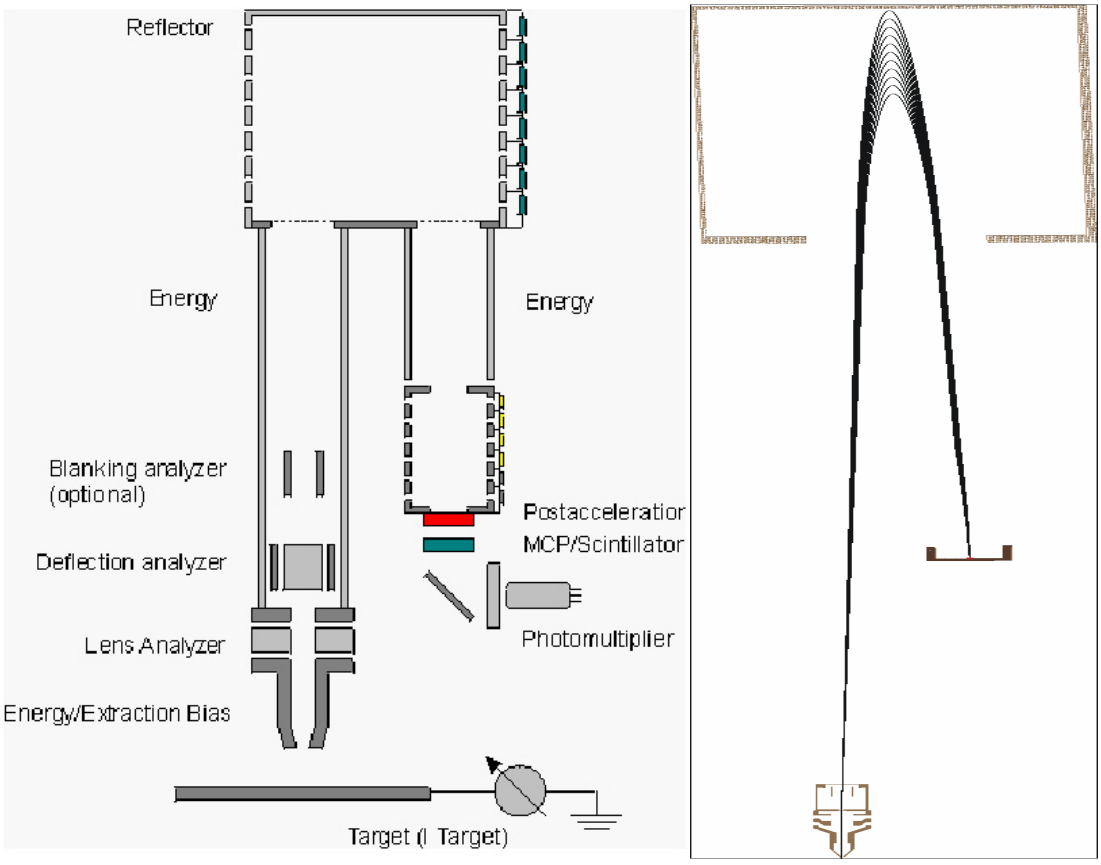

Figure 7: Mass analysing system of the ION-TOF[5] instrument including a reflectron [20]

The reflectron applies an electrical field with repulsive electrostatic force onto the incoming ions [21]. Ions with greater kinetic energy are

allowed to penetrate deeper into the reflectron against the repulsive electrostatic field until direction is reversed than ions with same mass but fewer kinetic energy and thus, have an elongated flight path. So, ions penetrating deeper will take more time to hit the detector, and therefore ions of one pulse set of a given equal mass-to-charge ratio but varying kinetic energies will reach the multichannel plate of the detector all at the same time [14], which means ideally, it imparts the same kinetic energy on all ions in the packet. Then, these ions are directed to drift through a field free region where the difference in velocities spatially separates ions of differing mass-to-charge ratio.

This way the reflectron decreases the spread in flight-times and mass resolution of the spectrometer is improved. For low voltages of the reflectron secondary ions can collide with the analyzer top ceiling, and can this way decrease signal intensity. This method requires pulsed ionization methods but has high ion transmission and the highest practical mass range of all mass spectrometer analyzers.

For dynamics SIMS instruments with higher primary current density other analyzers like magnetic sector, quadrupole, or trapped-ion mass analyzers are used.

3.4.4 SIMS Methods

Secondary ion mass spectrometry can be used for many different analytical procedures. For the different tasks the ION-TOF[5] instrument provides a variety of operational modes. Each has other main objectives for fitting the analytical problems and difficulties confronted with.

Surface Spectroscopy

This static SIMS investigation has the aim of examining genuine, non-modified surfaces and its composition. Surface Spectroscopy provides detailed elemental and molecular information from the outermost monolayers. As SIMS is in principle a destructive analysis technique secondary ion contribution from already bombarded surface should be negligible compared to newly acquired ion data. Through the application of very low primary ion dose densities this quasi non-destructive surface analysis can be achieved.

Therefore, only the Bi-cluster gun is used. To get elemental and molecular information of the surface the primary ion current density is very low. Thus, only a small fraction of a monolayer is removed during this analysis method. It results in an entire secondary ion mass spectrum with chemical information obtained each time a pulse of primary ions reaches the target sample. Via molecular and cluster ions very high sensitivity in the ppm and ppb range and high mass resolution and accuracy are achieved.

Surface Imaging

For this mode also only the liquid metal ion gun is operated. The primary ion beam consists of laterally focussed ion pulses and this primary beam is scanned over a square region of the surface of the sample. The lateral resolution of the element mapping is only dependent of the primary beam diameter.

This way, mass resolved maps of the regions of interest can be generated if the spectral information is combined with the spatial origin of the secondary ions. The mass spectrum and secondary ion images can then be used to determine the composition and distribution of sample surface constituents.

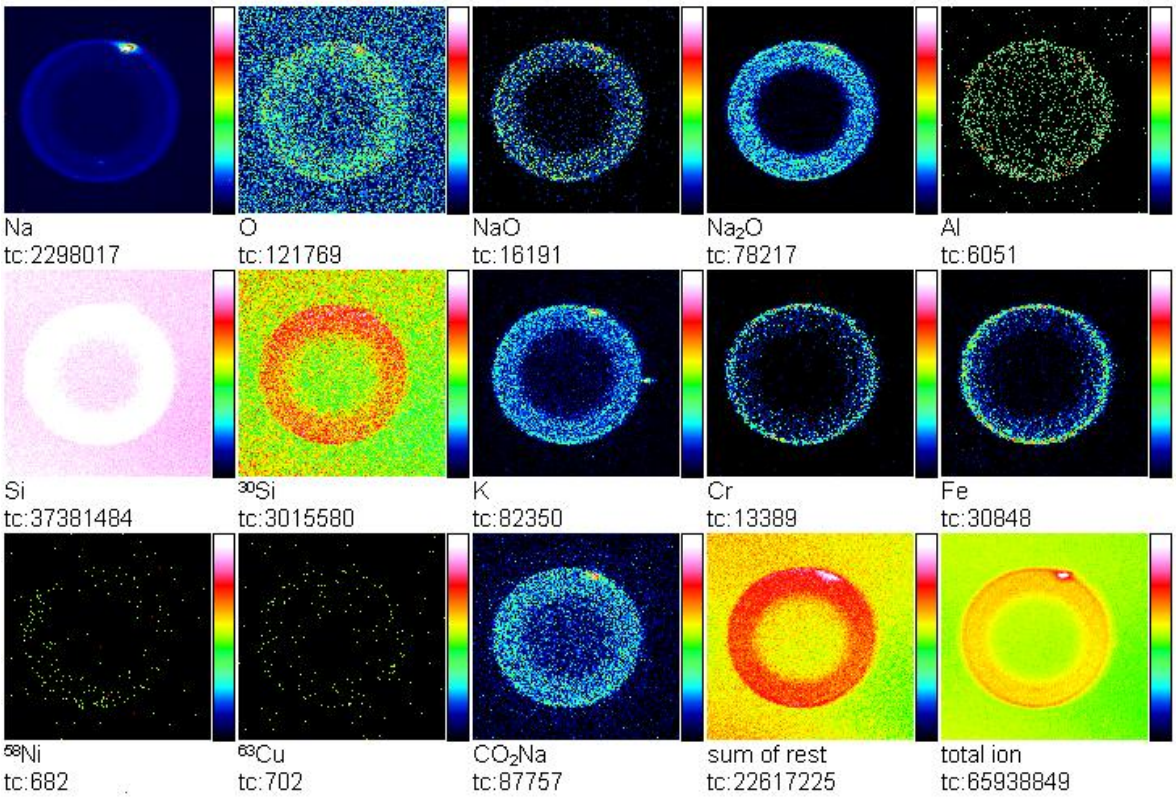

Figure 8: **Elemental mapping of a sodium carbonate solution droplet on silicon; annealed at a temperature of 280°C**

The colour-coded intensities of mass intervals of different elements result in an image of the secondary ions across the sample surface. This method has a high lateral resolution of less then 100 nm and mapping of all elements and isotopes simultaneously is possible. Another mode of operation allows the acquisition of the entire mass spectrum from every pixel in the image.

Depth Profiling

For depth profiling the TOF-SIMS instrument is operated in the Dual Beam Mode as for depth profiles in static SIMS a second ion beam is necessary to be rastered over the surface. While one beam progressively analyzes the crater bottom, another high current beam is applied to erode the sample surface leading to a sputter crater.

Usually static SIMS only removes sub-monolayer amount of surface atoms, due to its high sensitivity. Now, in addition a second, low energy sputter ion source is applied and continuously sputters layer by layer from the target sample's surface. The sputter raster of the high current ion beam is much bigger than the area in the centre of the crater that is actually analyzed by the LMIG beam, which generates the secondary ions to be measured. Thus, a depth profile of a sample may be obtained simply by recording sequential SIMS spectra as the surface is gradually eroded away by the incident ion beam probe. The raw data file of the depth profile stores the full information of the measurement related to the measuring time together with the lateral coordinates of the corresponding primary pulse. A plot of the intensity of a given mass signal as a function of time is a direct reflection of the variation of its concentration with depth below the surface.

The aim of depth profiling is to obtain information on the variation of composition with depth below the initial surface. Such information is obviously particularly useful for the analysis of layered structures such as those produced in the semiconductor industry.

One of the main advantages that SIMS offers over other depth profiling techniques like Auger depth profiling is its sensitivity to very low concentrations of elements. Again, this is particularly important in the semiconductor industry where dopants are often present at very low concentrations. It is also ideally suited for insulators.

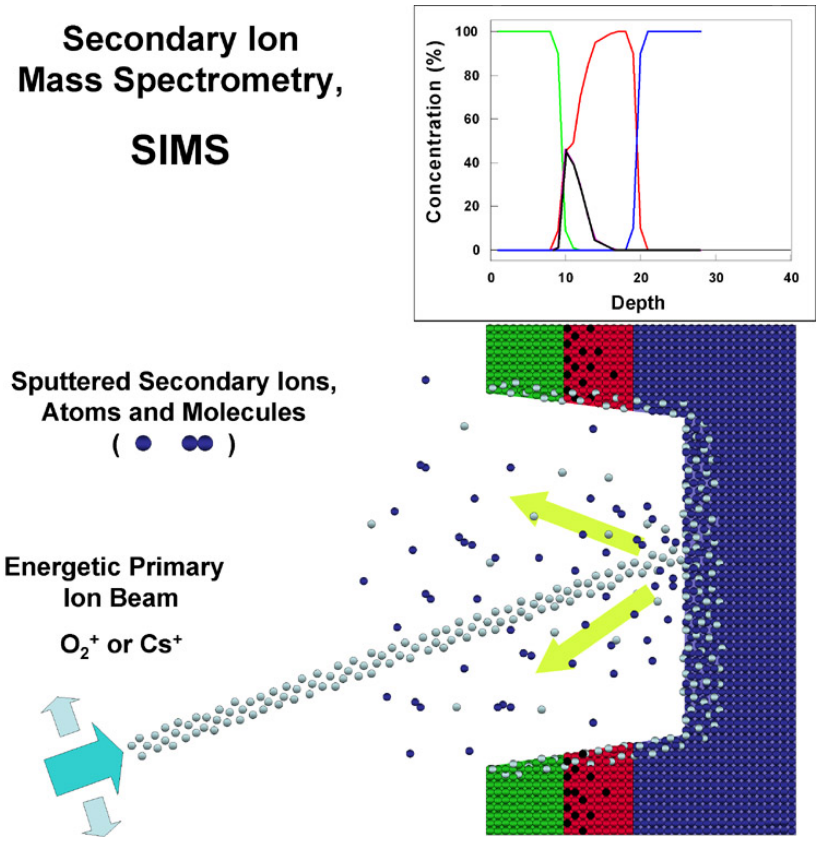

Figure 9: Depth profiling using SIMS

Prerequisites for sputter depth profiling include a flat crater bottom, in the sense of both a macroscopic curvature of the sample and the roughness on a micro scale on the crater bottom.

The depth resolution achievable is usually better than 1nm with very high mass resolution and fast sputter speeds of up to 10µm/h. It depends mainly on the atomic mixing, which occurs as primary ions reach an average depth until they are stopped through several collisions with sample atoms. Depending on mass, energy and impact angel also sample atoms are moved from their initial locations resulting in an atomic mixing in the surface near region. This limiting of the depth resolution is primarily caused by the sputter beam, whereas the amount of atomic mixing introduced by the analysis beam is negligible because it is constantly removed by the sputter beam's progression to greater depths.

3D-Analysis

The decoupling of sample erosion and secondary ion generation in the TOF-SIMS method also allows it to combine spectral, imaging and depth information to visualize laterally resolved three-dimensional sample structures. With this feature it is possible to plot elements and molecular distributions of the scanned volume and this makes it a powerful tool for the investigation of inclusions and complex or unknown buried structures of defects. In particular, the visualization of shape and positions of composition of features in the sample can easily be achieved.

3.4.5 Concentration Calibration

In SIMS measurements the acquired information is the intensity of the secondary ions removed from the surface. These intensity profiles have to be converted into analytical concentrations.

The intensity of secondary ions of a chosen mass and the reliance to specified parameters of the SIMS operation is given by the following equation:

$$I_{S_n(A)} = I_P \cdot Y_{tot} \cdot c_A \cdot i_{n(A)} \cdot \alpha_A^{\pm} \cdot \eta_A .$$

$I_{Sn(A)}$ secondary ion intensity of the measured isotope n of the element A [secondary ions/s]

I_P primary ion beam intensity [primary ions/s]

Y_{tot} total sputter yield [atoms/primary ion]

c_A concentration of the element A in the sample

$i_{n(A)}$ isotope fraction of the measured isotope n of element A

α_A positive respectively negative ionisation probability of the element A

η_A measurement efficiency of the secondary ion mass detection (output of the ion extraction, transmission factor of the spectrometer, efficiency of the detector)

For additional calibration of the depth scale the altitude of the sputter crater is measured afterwards by a stylus profilometer since this is not possible during depth profiling. For homogeneous silicon wafers

the sputter rate usually is assumed to be constant throughout the whole measurement of the profile. But for multilayer systems this is not the case and can lead to distorted results.

Relative Sensitivity Factor

Since the ionisation probability is not only dependent on the element itself but is also dependent on the chemical surrounding and matrix effects quantification of SIMS data can only be achieved by the use of standards with known amounts of the same matrix-impurity combination. The intensity of the impurity is scaled to the standards by a relative sensitivity factor (RSF) [23]. Standards have to be measured under identical experimental conditions. The secondary ion yield due to chemical enhancement varies if for instance the electropositive element caesium is present in the uppermost layer of the surface, which would increase the yield of negatively charged secondary ions or if amounts of electronegative oxygen change the oxidation state in the transient region to a higher yield of negative secondary ions.

The use of standards of similar condition and known content is definitely the most accurate quantitative method. The relative sensitivity factor [24] provides the correlation between the ratio of impurity signal intensities to concentration of the reference element $\frac{c_{el}}{c_{ref}}$ and the ratio of the corresponding measured intensities $\frac{I_{el}}{I_{ref}}$ which is defined by the equation:

$$\frac{I_{el}}{I_{ref}} = RSF \cdot \frac{c_{el}}{c_{ref}}$$

Several parameters can change significantly due to instrumental instabilities and small variations of the instrument setup. By the use of the relative sensitivity factors this can be overcome. The RSF is defined as relation between the intensities of an element A to the matrix element M leading to following equation:

$$\rho_{A/M} = \frac{I_P \cdot Y_{tot} \cdot \alpha_A^{\pm} \cdot i_{n(A)} \cdot \eta_A}{I_P \cdot Y_{tot} \cdot \alpha_M^{\pm} \cdot i_{n(M)} \cdot \eta_M} = \frac{I_{S_n(A)} \cdot c_M}{I_{S_n(M)} \cdot c_A}$$

$\rho_{A/M}$ relative sensitivity factor (RSF)

$I_{Sn(A,M)}$ secondary ion intensity of the measured isotope n of the element A and element M, respectively [secondary ions/s]

I_P primary ion beam intensity [primary ions/s]

Y_{tot} total sputter yield [atoms/primary ion]

$c_{A,M}$ concentration of the elements A and M, respectively in the sample

$i_{n(A,M)}$ isotope fraction of the measured isotope n of the elements A and M, respectively

$\alpha_{A,M}$ positive respectively negative ionisation probability of the elements A and M, respectively

η_A measurement efficiency of the secondary ion mass detection (output of the ion extraction, transmission factor of the spectrometer, efficiency of the detector)

Two kinds of standards can be distinguished. Homogenous standards for relatively simple calculations for high convenience and inhomogeneous standards easily prepared by implantation. For these inhomogeneous implantation standards the RSF value can be determined from the sum of concentrations in each depth over the whole implantation range, which corresponds to the entire implantation

dose of known value. Thereby, it is assumed, that the implantation does not change the concentration of the matrix element and that the RSF can be considered constant over the whole concentration range, recommending relatively low concentrations of implanted atoms using this method. This leads to:

$$\rho_{A/M} = \frac{\sum_{i=1}^{z} \frac{I_{S_n(A)(i)}}{I_{S_n(M)(i)}} \cdot d}{Q_d \cdot z}$$

z number of cycles

$I_{Sn(A,M)(i)}$ secondary ion intensity of the measured isotope n of the element A and M, respectively [ions/s]

d crater depth [cm]

Q_d implantation dose [atoms/cm^2]

Finally the concentration of the impurity can be calculated after deriving the RSF from standards and determining the ratio of secondary ion intensities:

$$c_A = \frac{I_{S_n(A)} \cdot c_M}{\rho_{A/M} \cdot I_{S_n(M)}}$$

4 Experimental Setup

4.1 Sample Preparation

4.1.1 Copper Gettering Samples

The samples for investigation of copper gettering effects were all prepared in the Forschungszentrum Rossendorf in Dresden. All together eight samples were prepared for measurements. Four of them were implanted with oxygen ions, each with an energy of 200 keV. Two more samples were prepared by implantation of phosphorous ions with an energy of 450 and 200 keV, respectively. The last two samples had Si^+ ions implanted, each with an energy of 450 keV. For implantation, ion doses of $3x10^{15}$ions/cm^2 for oxygen implant ions and $1x10^{15}$ions/cm^2 for phosphorus and silicon ions were applied.

The silicon wafer was a (1 0 0)-oriented, n-type Czochralski-Si. Four of the samples were doped by especially high boron concentrations. Implantation was done at an angle of 7° with respect to the surface normal. This odd numbered angel is used to avoid channelling effects of the ions through the crystal lattice. This phenomenon occurs when the target material is monocrystalline. Then, the yields of physical processes after a charged particle is incident upon a solid target are very strongly dependent on the orientation of the momentum of the particle relative to the crystalline axes or planes. This effect is commonly called the "channelling" effect.

All the samples were furnace annealed at temperatures of 1000°C under argon conditions. Two oxygen implanted wafers were annealed for 240 min, whereas the six others were tempered for 30 min.

In a second step copper was implanted into the backside of each sample. Here, impurity atom implantation doses were $3x10^{13}$ ions/cm^2 at an energy of 20 keV. The samples were then annealed using rapid thermal annealing at 700°C for 120s to diffuse the contamination atoms throughout the wafer bulk. For samples 1Bb, 1Ba, PB, and SB the silicon wafer was exceedingly doped by boron atoms.

Sample	Implantation dose [ions/cm^2]	Implantation energy [keV]	Annealing conditions [°C / min]
1Ab	3e+15	200	1000 / 240
1Bb	3e+15	200	1000 / 240
1Aa	3e+15	200	1000 / 30
1Ba	3e+15	200	1000 / 30
P	1e+15	450	1000 / 30
PB	1e+15	200	1000 / 30
S	1e+15	450	1000 / 30
SB	1e+15	450	1000 / 30
Cu-Std	6e+14	1400	900 / 0,5

Table 2: List of sample parameters as provided by the Forschungszentrum Rossendorf, Dresden

4.1.2 Sodium Diffusion Samples

For the subsequent investigation of sodium surface diffusion two solutions were prepared. In the first solution sodium acetate (CH_3COONa) was used and for the other one sodium carbonate (Na_2CO_3) was dissolved; each in concentrations of 10^{-4} mol solute per mol solvent. As solvent ultra pure water for trace element analysis from a Millipore 'Milli-Q' system was used.

Originally, sodium hydroxide solutions were considered but as they would easily dissolve atmospheric carbon dioxide from air into sodium carbonate, hence a sodium carbonate solution was used. The reasons to choose sodium acetate as sodium donor molecule were its low ionic binding energies. In contrast to the organic acetate molecule, the inorganic sodium iodide molecule with low binding energies as well should also be investigated. Furthermore, sodium oleate for regular thin coating was in consideration but setbacks with the TOF-SIMS instrument did not allow further investigations in time.

For investigations of the diffusion from sodium molecule contamination the solutions were applied onto the silicon wafer surface by the use of a 0.5 µl Hamilton-syringe. The blunt and evenly shaped tip with an outer diameter of 0.5 mm was sand grinded to form it to a conical shape around the aperture for less contact area of the droplet to tip. The droplets were then applied onto the surface under a microscope.

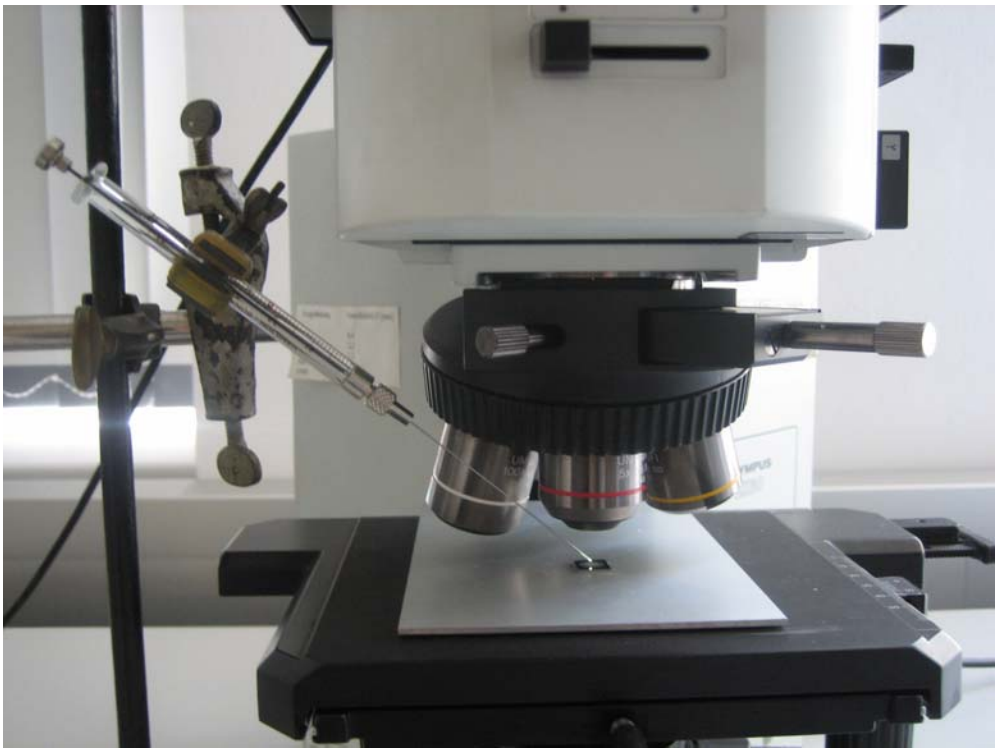

Figure 10: Setup for applying droplets onto the silicon wafer surface by the use of an Hamilton-syringe under an microscope

The maximum diameter for measurements with the ION-TOF[5] instrument is 500x500 µm. Thus, the droplets had to be made as small as possible to be able to raster over the entire droplet. Eventually, the spreading droplet wetting the surface could be produced slightly smaller than the width of the analyzing window of the TOF-SIMS.

Diffusion effects were investigated for different temperatures ranging from room temperature up to 280°C, 450°C, 600°C, and 750°C. All thermal annealing procedures were carried out under argon atmosphere using furnace annealing for a period of 30 min.

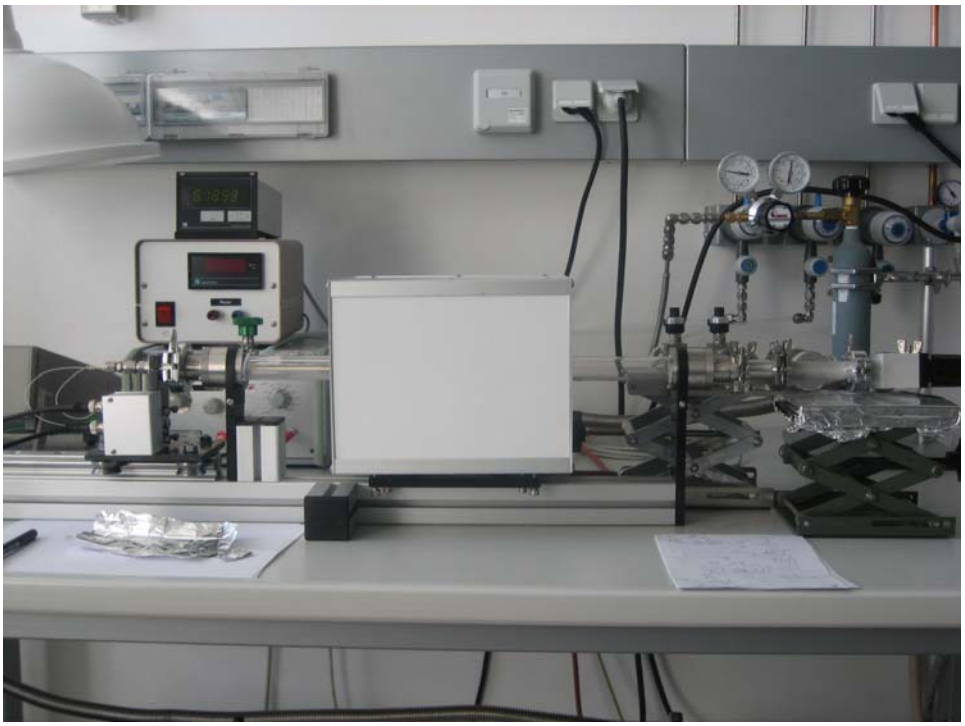

Figure 11: Furnace equipment for thermal annealing treatments

4.2 Ion implantation Simulations

The simulations for implantation of the defect creating atoms were carried out with the SRIM (Stopping and Range of Ions in Matter) program. This calculation uses a full quantum mechanical treatment of implantation-ion-to-bulk-atom collisions. Included in SRIM is the TRIM (TRansport of Ions in Matter) program. This program predicts amongst others the production of vacancies and the implantation range of the atoms strongly depending on their mass, the angle of incidence, and especially the implantation energy.

The TRIM program is a Monte-Carlo calculation, which in detail calculates the energy transfer from the incoming ion to target atoms during collisions [22]. All target atom cascades in the sample are

computed separately. In TRIM simulations compound materials of up to eight layers, each consisting of separate materials could be processed. Both, the final three dimensional ion distribution and also all associated phenomena to the ion's energy loss, including target damage, ionisation, and phonon production can be evaluated.

All the target atom cascades in the sample are individually calculated and recorded. For these simulations a number of 10 000 impinging atoms was determined at an implantation angle of 7°. Each atom creates vacancies while hitting the sample and advancing through the bulk.

For the copper gettering investigations three different implantation ions were used. For each atom the vacancy distribution and the transport range in the sample were computed.

The maximum in the ion ranges represents the area where most implantation atoms come to a rest as interstitial atoms. During the first thermal treatment step of the sample preparation these interstitials can combine with the vacancies. Remaining vacancies which are able to act as gettering sites will be well departed from the projected ion range.

For different implant atoms the differences in ion ranges can be clearly distinguished. At same energies of 200 keV the projected ion range for oxygen ions has a maximum at a depth of 440 nm whereas for phosphorus ions at this energy gather to a maximum at 260 nm. The same implantation atom has evidently reached greater depths as the energy is increased to 450 keV. For phosphorus atoms penetration depth changes from 260 nm to deeper regions of around 560 nm. Silicon ions at implantation energies of 450 keV gather as self-interstitials in the silicon wafer in the range of 590 m.

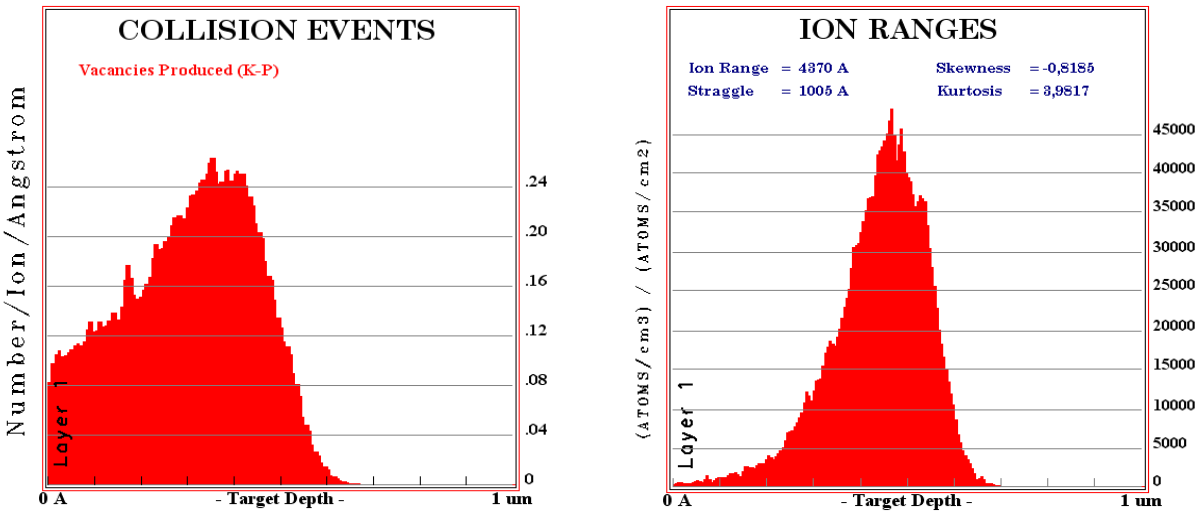

Figure 12: **Implantation events after oxygen ion implantation at 200 keV**

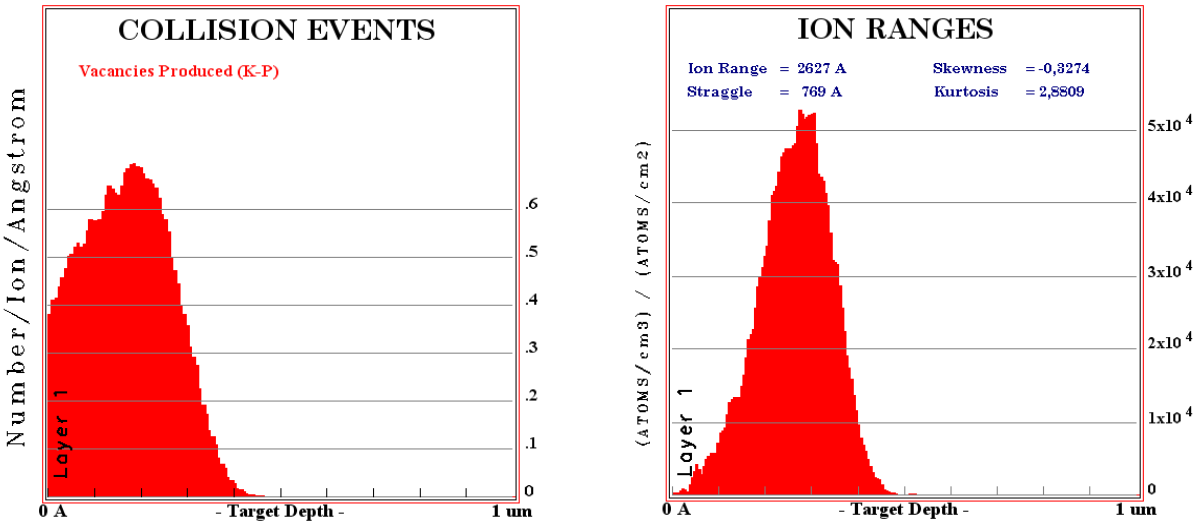

Figure 13: **Implantation events after phosphorus ion implantation at 200 keV**

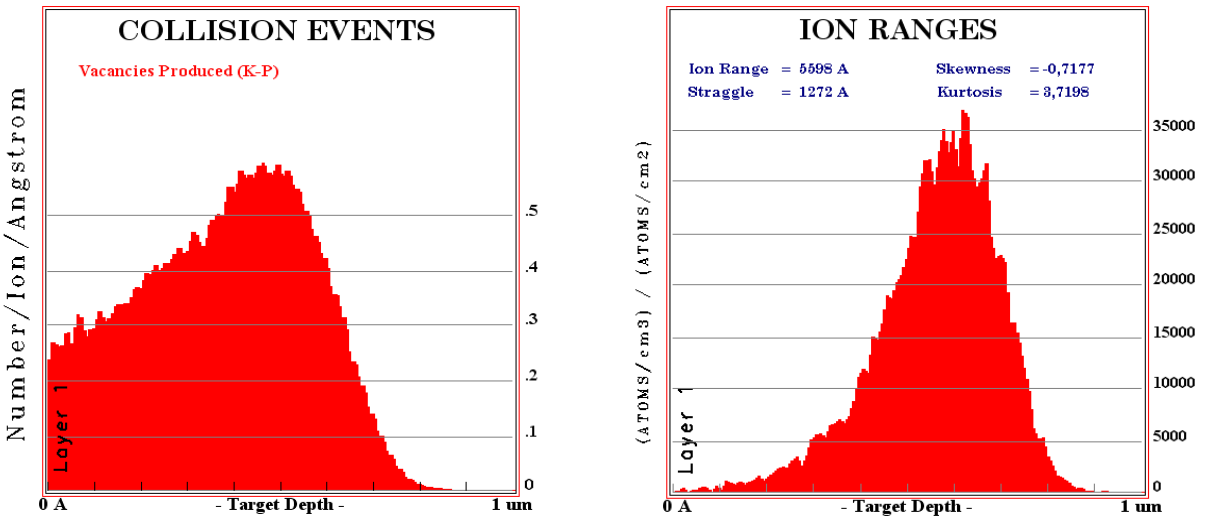

Figure 14: **Implantation events after oxygen ion implantation at 450 keV**

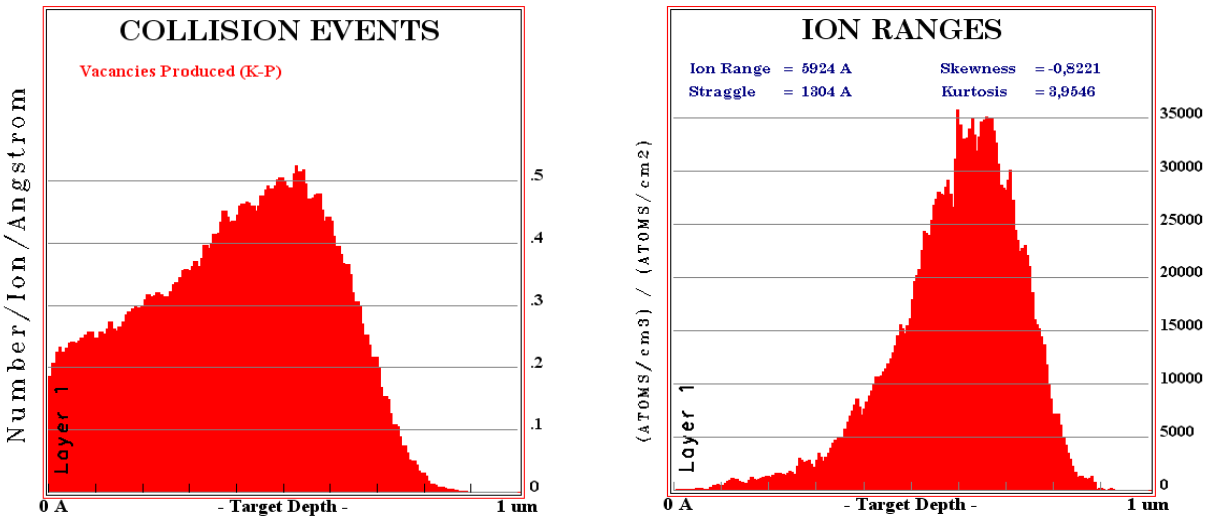

Figure 15: **Implantation events after silicon ion implantation at 450 keV**

Measurement Conditions

On the TOF-SIMS instrument many parameters can be adjusted to the needs of the analytical problem at hand. For all measurements the Bi ion gun was loaded in the *high current bunched mode* using and energy of 25 keV. This analysis gun was fairly unstable at times due to its operation during an already long lasting lifespan. The Bi emitter finally had to be changed during investigation of sodium diffusion.

Figure 16: ION-TOF[5] instrument of the TOF-SIMS research group at the TU Wien

The depth of all sputter craters was measured by the use of a Sloan Dektak IIA device in the 'average height' mode. This instrument uses a stylus profilometer to determine variations in depth.

4.2.1 Copper in Silicon

Each sample has been measured with the ION-TOF^5 instrument. All four samples implanted with oxygen were investigated in positive and negative mode. The other four samples with two implanted by phosphorus ions and two by silicon ions were measured only in positive mode.

In negative mode more negative secondary ions are extracted by the extractor field and in positive mode significantly more emission of negative secondary ions is promoted. For the negative mode Cs sputtering was used as for the positive mode the O_2 sputter gun was applied. The sputter ion gun was set to an energy of 1 keV and the current of the ion beam was adjusted to a target current of 250 nA for oxygen sputtering and to 115 nA for the Cs sputter gun.

The analysis gun was loaded in high current bunched mode and set to Bi_1^+ ions with energies of 25 keV. The field of view of the Bi ion gun was set to 102.5x102.5 µm while the sputter raster used had an area of 300x300 µm to avoid crater side effects. For these measurements cycle times of 30 µs were used limiting the mass spectra to around 80 amu.

4.2.2 Sodium in Silicon

All depth profiling measurements for sodium in silicon were done only in positive mode with oxygen primary ions as sputter beam. The sputter ion energy was 2 keV with an ion current of close to 600 nA.

The rastered area for sputtering was a square of 800x800 µm, whereas the area scanned by the liquid metal ion gun for analysis was of a square of 500x500 µm. All of these secondary ion spectra were measured using Bi_1^+ ions with a cycle time of 40 µs to gather information of ions of masses up to 140 amu.

4.2.3 Cu - Standard

To quantify the results of SIMS measurements standards of the same composition are essential. Therefore, under the same conditions as the samples a copper standard has been measured. The copper standard is also an implantation standard. It has been previously used for the investigation of Cu gettering effects in silicon by this group of research.

Like the samples, the standard has also been produced by the Forschungszentrum Rossendorf with the aim to obtain a maximum concentration of $1x10^{19}$ atoms /cm^3. Implantation energy for the standard was 1.4 MeV with an ion dose of $6x10^{14}$ atoms/cm^2.

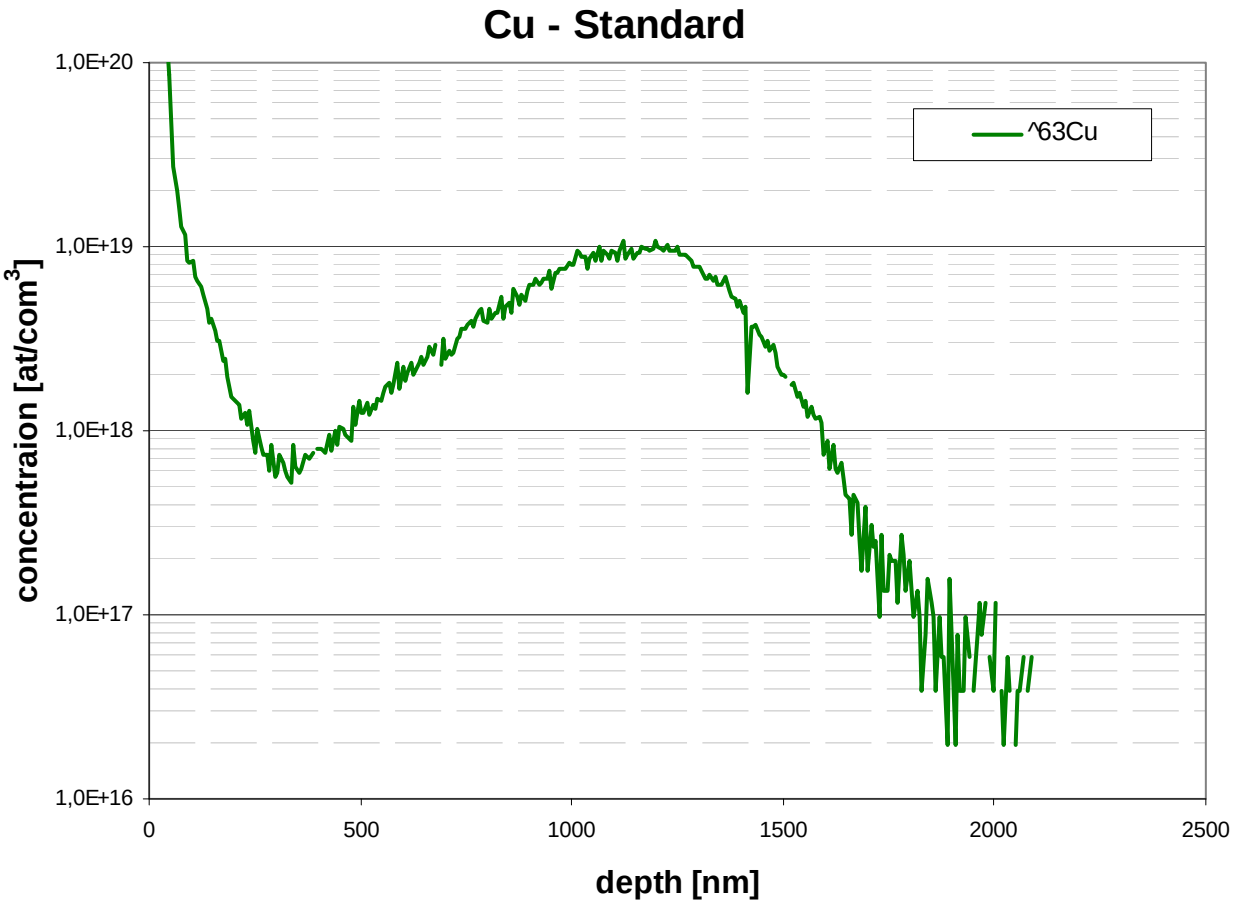

Figure 17: **Copper implantation standard depth profile**

5 Results and Discussion

The clearly visible enrichment of copper and other components towards the surface can partly be explained as an artefact of SIMS measurements. Native oxide layers present on the surface are acquired in oxygen containing atmosphere as well as under higher temperatures during thermal annealing phases. These are able to change to ionisation probability of surface atoms, which results in an increase of the signals of secondary ions of origin close to the surface. Crystal defects of the top surface layers are also a natural sink for impurities leading to enriched signal intensities.

5.1 Cu-gettering in Silicon

5.1.1 Oxygen Ion Implants

First, series of depth profiles were done on samples implanted with oxygen ions at 200 keV. In preceding measurements attention was given to diffusion behaviour of P^+, Si^+ and As^+ ions in silicon [9, 12, 25-27]. Similar effects are now expected for O_2^+ ion implantation.

The first two samples were prepared using silicon wafers that were not doped with boron atoms. The oxygen gettering sites show a broad peak around the expected penetration depth of maximum congregation with matching intensities. Both peaks show similar shape and ion range though tempering times were varied from 30 (1Aa) to 240 min (1Ab). The copper gettering at the R_p range shows a strong peak, which is corresponding to the oxygen implantation range of about 440 nm. Only this gettering layer at R_p is visible as no other noticeable accumulations at an $R_p/2$ or trans-R_p range appear.

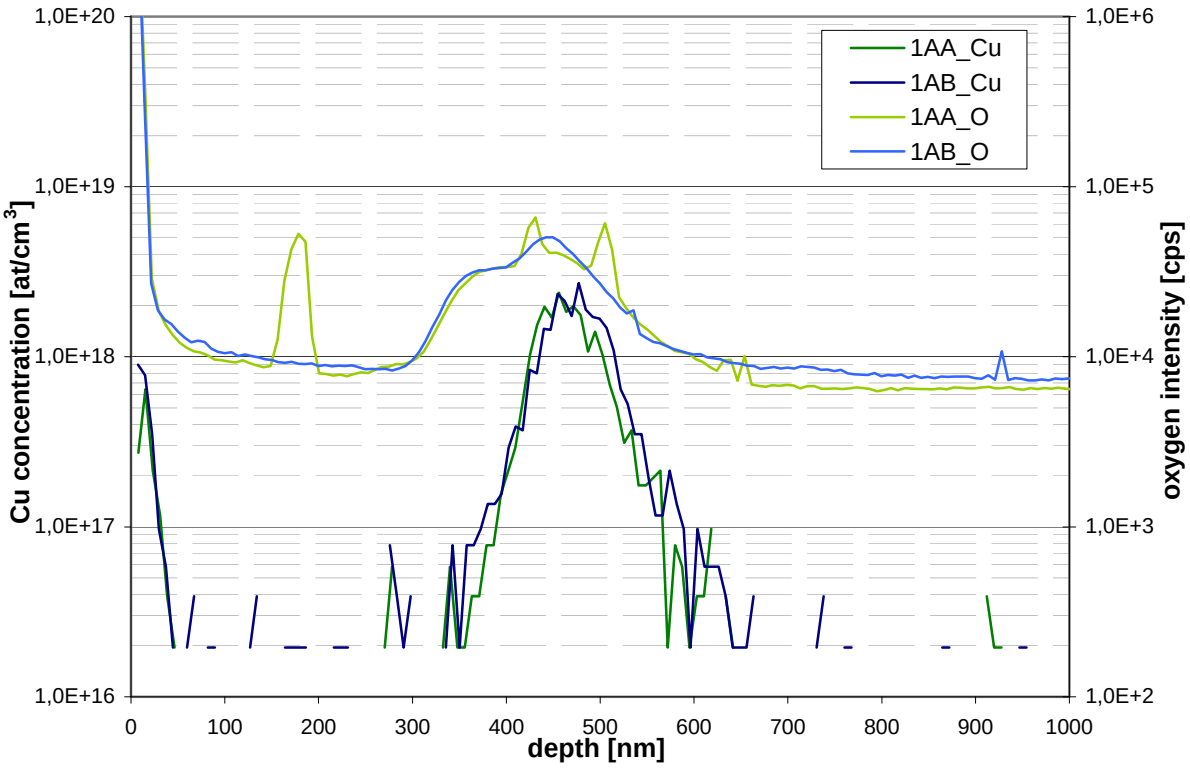

Figure 18: Depth profile of samples implanted by oxygen ions at 200 keV

One oxygen depth profile shows distinct, sharp peaks arising. These spikes originate from oxygen precipitates in the silicon wafer that occur during Czochralski-silicon production processes. The ^{18}O profile of sample 1Aa in Fig. 19 shows corresponding peaks to the spikes in the ^{16}O profile. This undoubtedly indicates atmospheric inclusions in the silicon since implantation was done only using ^{16}O atoms. In this spectrum at around 650 nm little spikes are obvious. These deviations are instrument artefacts as they derive from current fluctuations of the analysis ion gun.

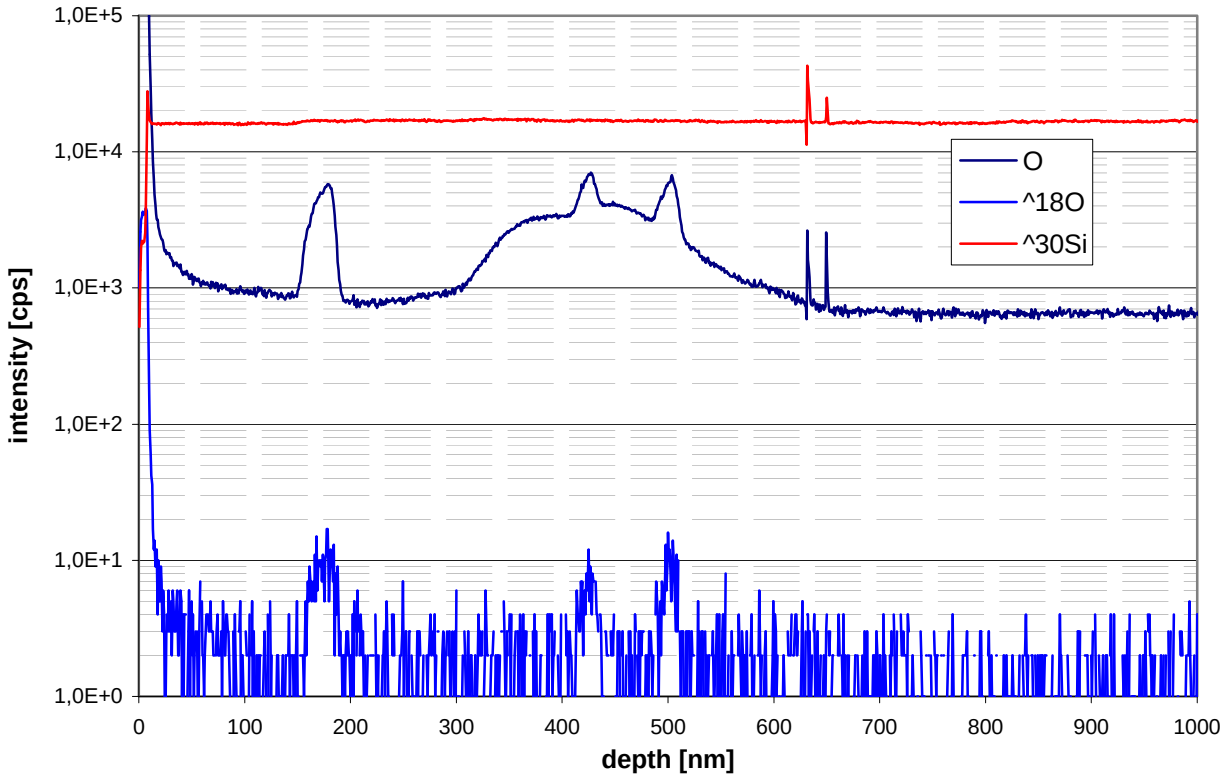

Figure 19: Oxygen distribution of sample 1Aa

The next two samples implanted with oxygen ions were highly doped with boron atoms and also annealed for 30 (1Ba) and 240 min (1Bb), respectively. Again, towards the surface an increase of concentrations of implanted ion species can be observed.

Sample 1Ba shows a maximum for oxygen slightly above the projected ion range of 440 nm. Furthermore, two more peaks occur of which one occurs at approximately half the projected ion range and to other in greater depths. The next sample 1Bb, annealed for four hours, does not show any gettering events for oxygen ions. One spike appears at about 260 nm but this can also be revealed as an inclusion of atmospheric oxygen in the silicon bulk.

Copper gettering effects for highly boron doped silicon show a broad band at very low concentrations. A strong copper peak is visible at surface layers descending rapidly in deeper regions. In regions of the projected ion range R_p and $R_p/2$, respectively no certain peaks can be distinguished. However, broad bands reaching into the trans-R_p range can be identified having a maximum at depths of about 650 nm. Concentrations for sample 1Bb of highly boron doped silicon show slightly higher amounts of copper and accumulation bands are shifted to slightly greater depths at a maximum at 700 nm for longer annealing times of 240 min.

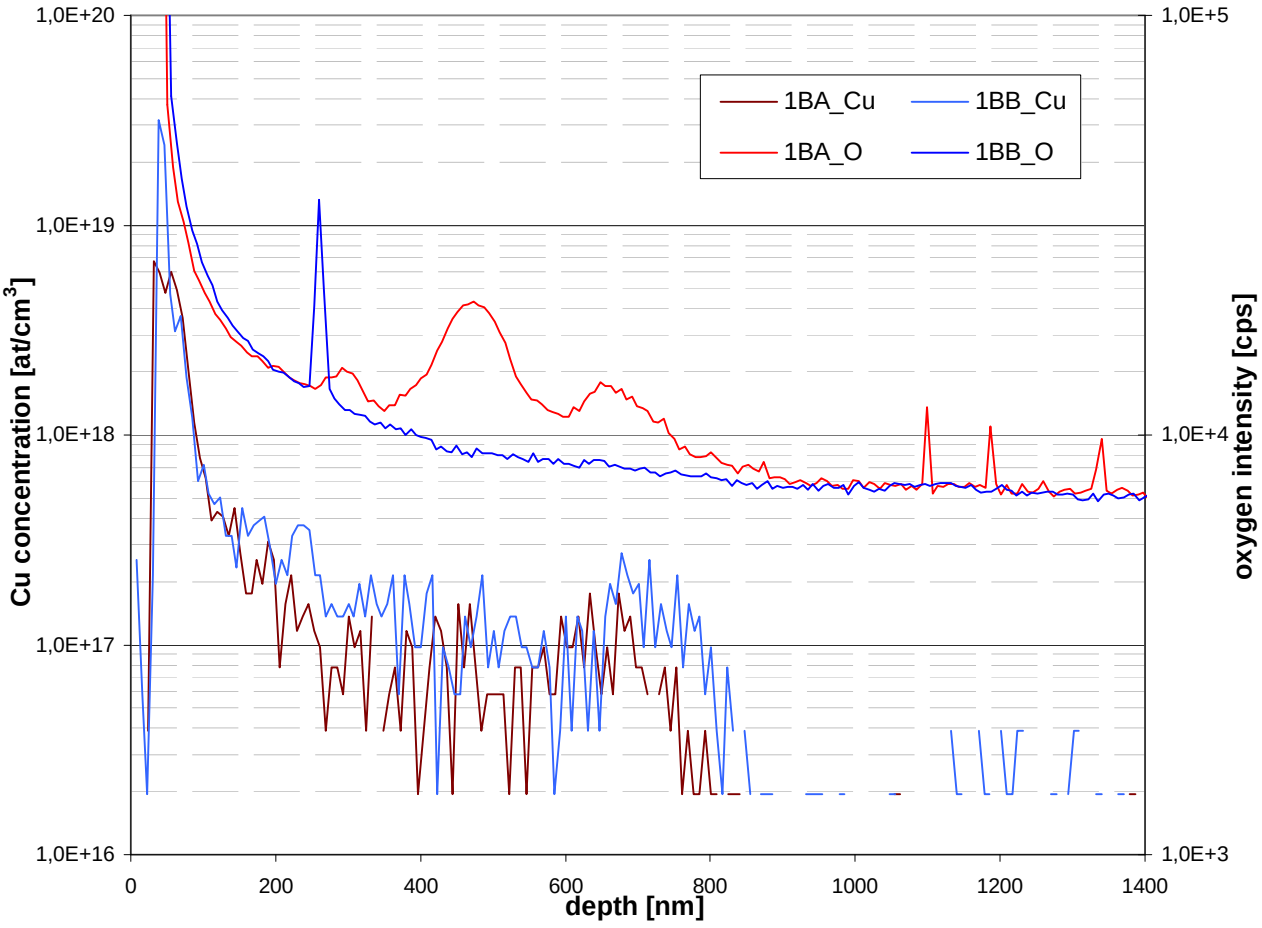

Figure 20: Depth profile of samples implanted by oxygen ions at 450 keV

A detailed view of the copper band is given in Figs. 21 and 22. Elevations at the trans-R_p range are accentuated via black lines. In Fig. 23 the shift of the trans-R_p bands of the boron doped samples after varied annealing times are indicated. FIG show the copper gettering effects individually for each sample in greater detail.

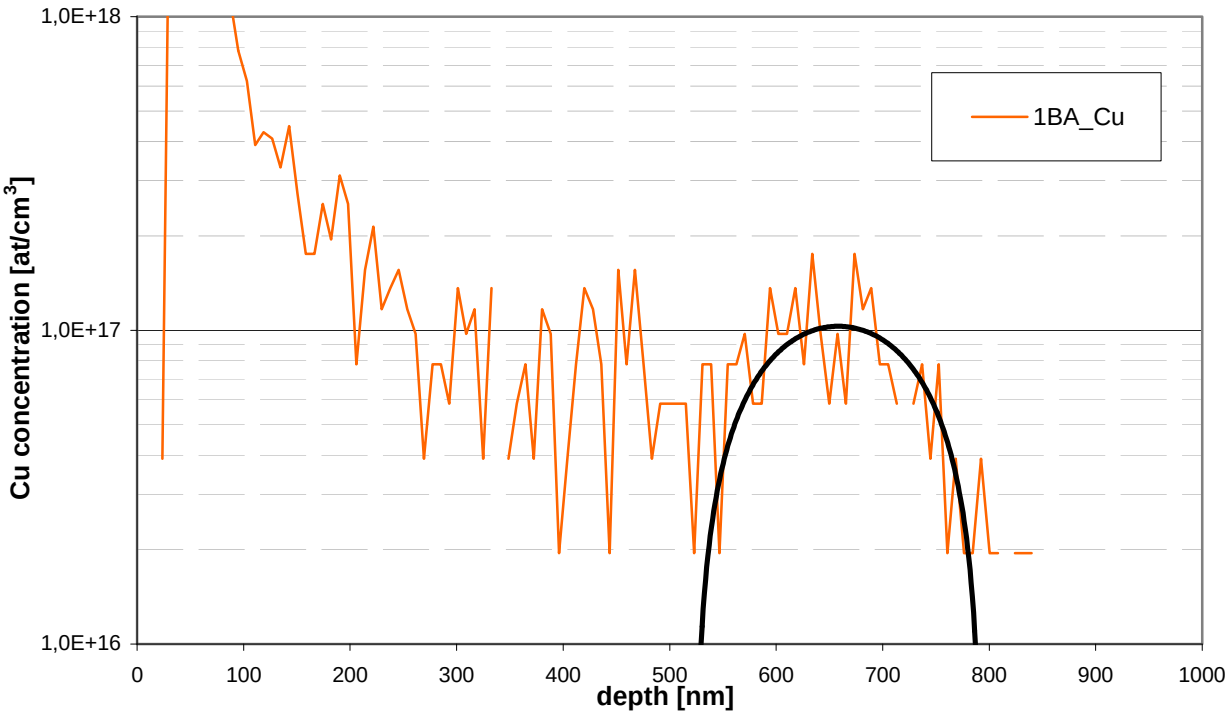

Figure 21: Quantified depth profile of sample 1Ba

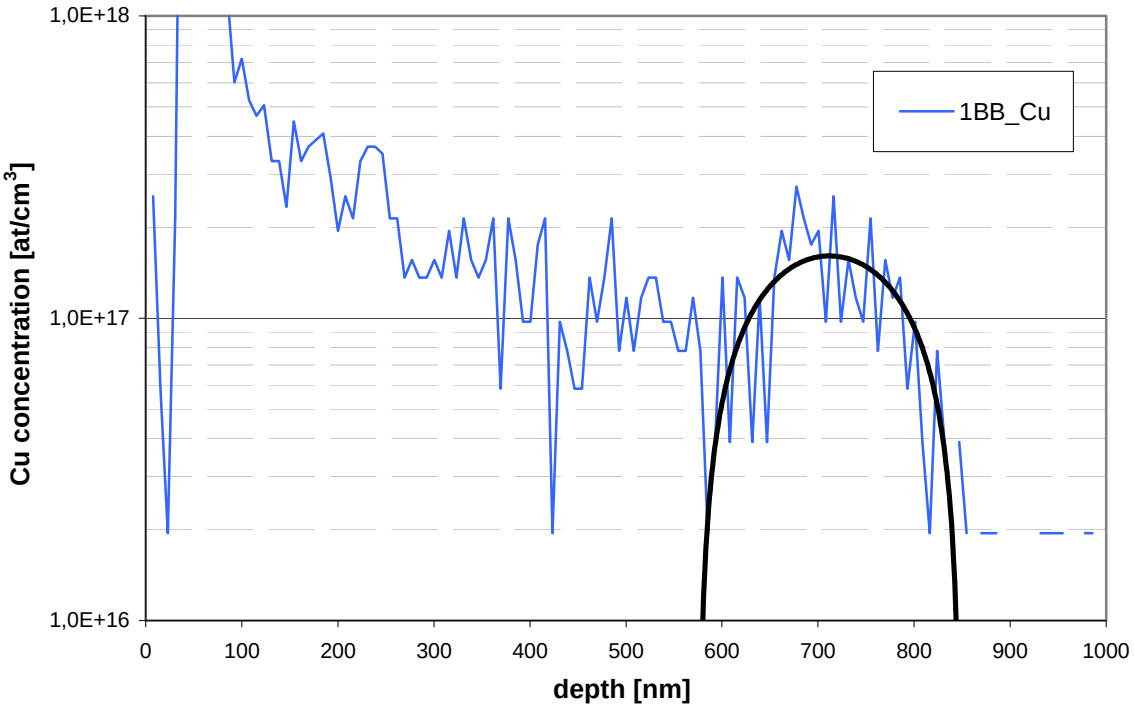

Figure 22: Quantified depth profile of sample 1Bb

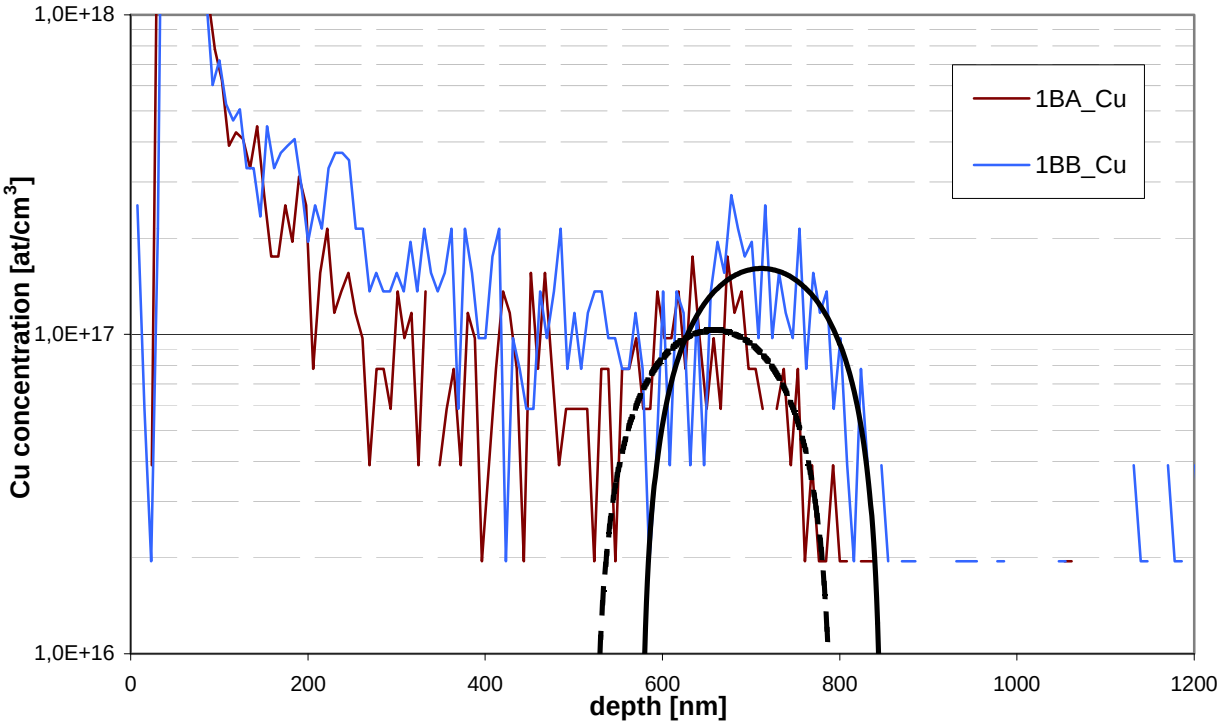

Figure 23: Shift of trans-Rp gettering after longer annealing times

In Fig. 24 also the boron atoms in the silicon bulk are included. At a depth of about 750 nm a rapid decline of boron is noticeable. Before the onset of the evident decrease, an increase in boron concentrations is visible. This boron accumulation corresponds to the depths of the trans-R_p bands of the copper gettering.

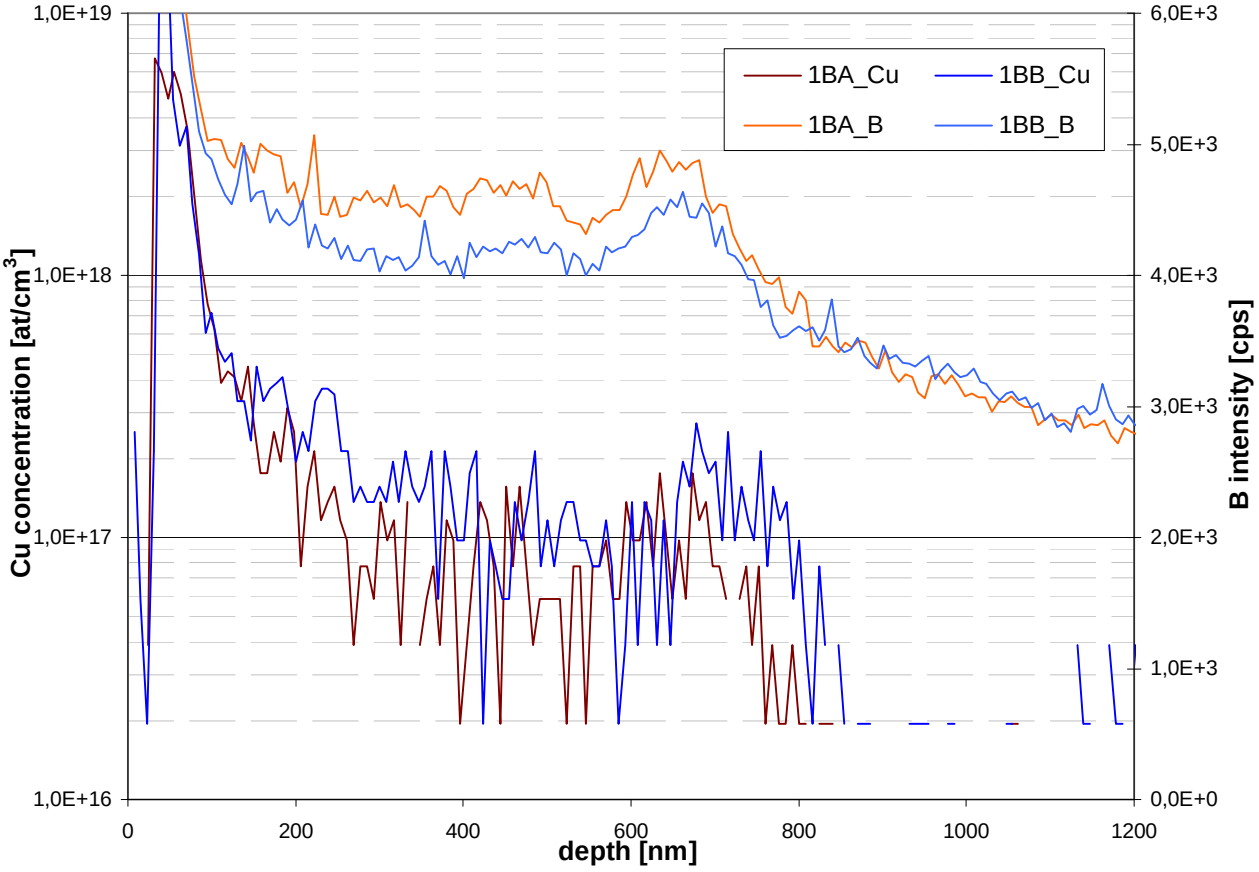

Figure 24: Depth profile of samples 1Ba and 1Bb including boron intensities

5.1.2 P^+ and Si^+ Ion Implants

Two samples were prepared using phosphorus as implant ion at different implantation two energies of 200 end 450 keV. The projected ion range simulated by TRIM for the case of 200 keV is 260 nm and for an energy of 450 keV it is 560 nm. Both samples show a very broad band for phosphorus ions having the maximum in the region of the expected ion range for 450 keV implantation. This would suggest equal implantation energy for both samples.

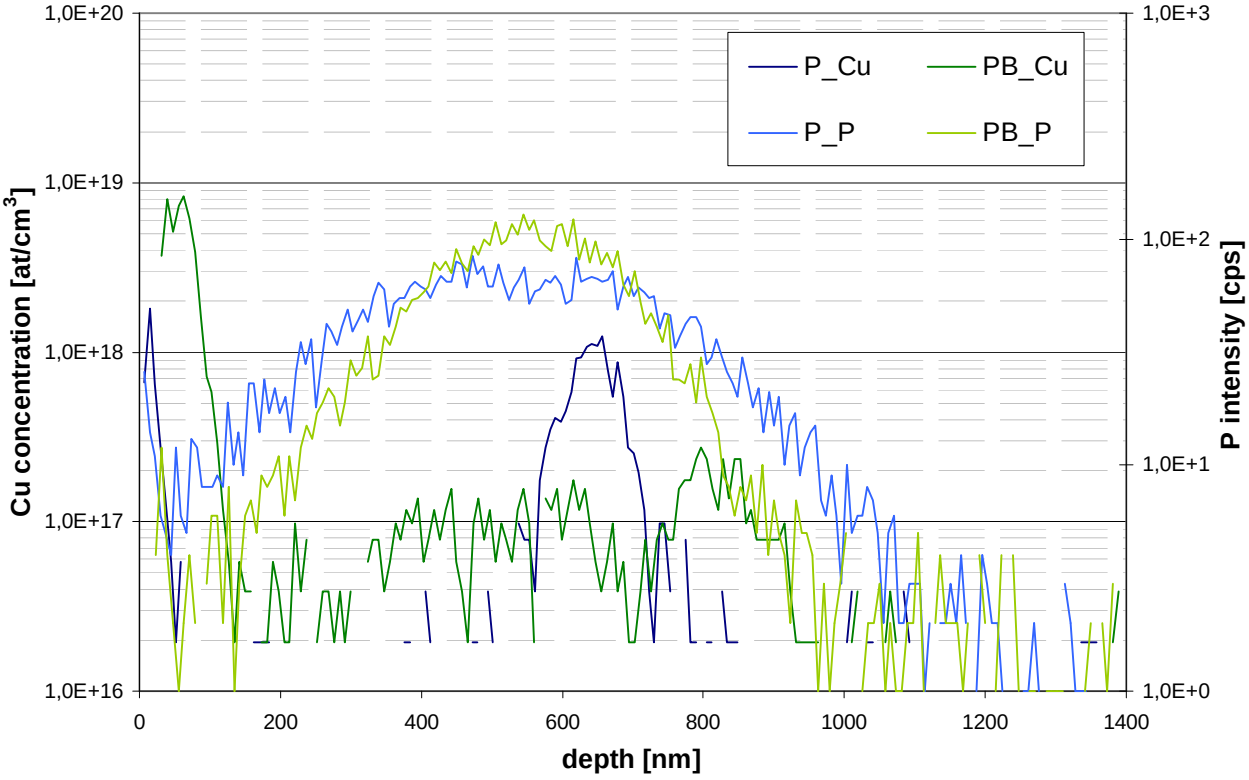

Figure 25: Depth profile of samples implanted by phosphorus ions

For sample P a significant peak is evident having the maximum slightly above 600 nm. This shift of copper gettering to greater depth possibly results from channelling effects during ion implantation allowing

atoms to penetrate deeper into the wafer bulk. Again, no other gettering effects in the $R_p/2$ or the trans-R_p range are observed.

Sample PB presents no such distinct peak but a broad band, as has been previously observed for boron doped samples. This broad band shows no distinguishable peaks for R_p or $R_p/2$ but stretches over a wide range, the implantation range for 450 keV in the centre. A more distinct peak shows in the trans-R_p region at around 800 nm. As well, this would lead to an implantation energy of 450 keV also for sample PB.

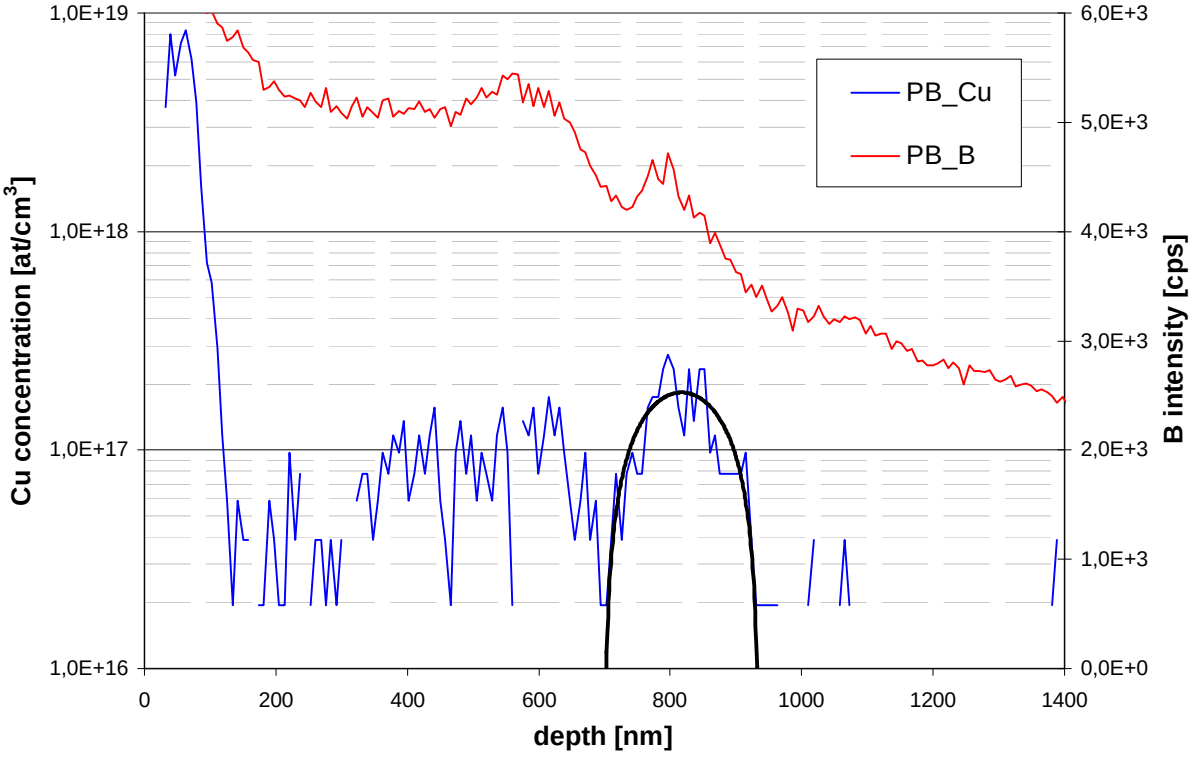

Figure 26: Quantified depth profile of sample PB including boron intensities

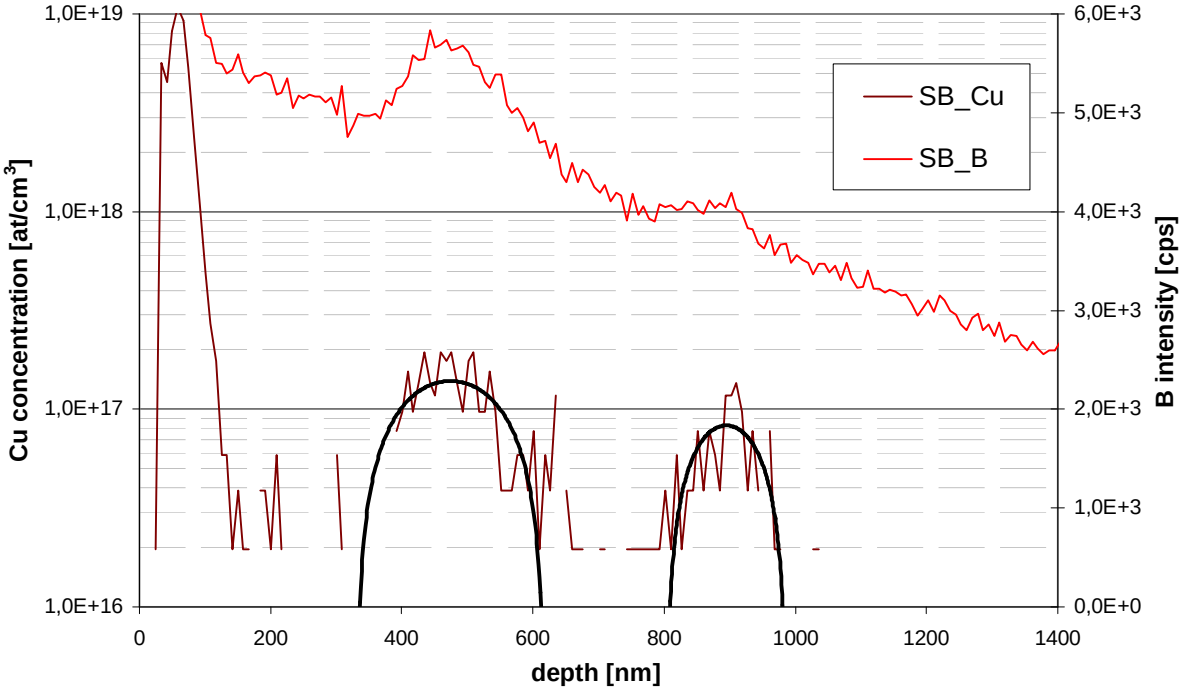

Figure 27: Quantified depth profile of sample SB including boron intensities

Including the boron intensities for sample PB it shows the strong decline in boron concentration as witnessed before. The trans-R_p region of the copper gettering corresponds to a slight deviation in the descending boron curve. Also, the boron doped sample SB, which was implanted by Si^+ ions, shows a Cu gettering zone at the R_p range and additionally one peak in the trans-R_p range at 900 nm with corresponding fluctuations in boron intensities.

Comparison of both boron doped samples shows Cu gettering bands at about the same R_p region but gettering in the trans-R_p region is clearly shifted to greater depths for sample SB.

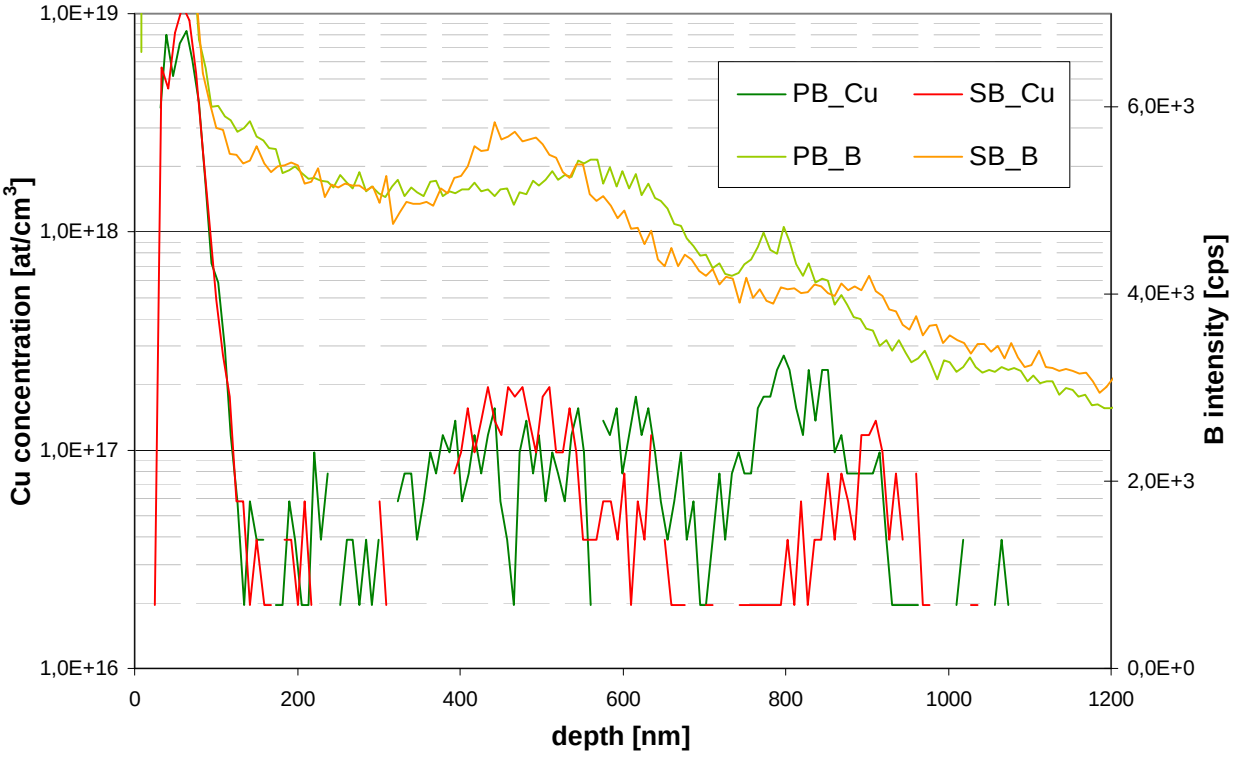

Figure 28: Comparison of depth profils of boron doped samples PB and SB

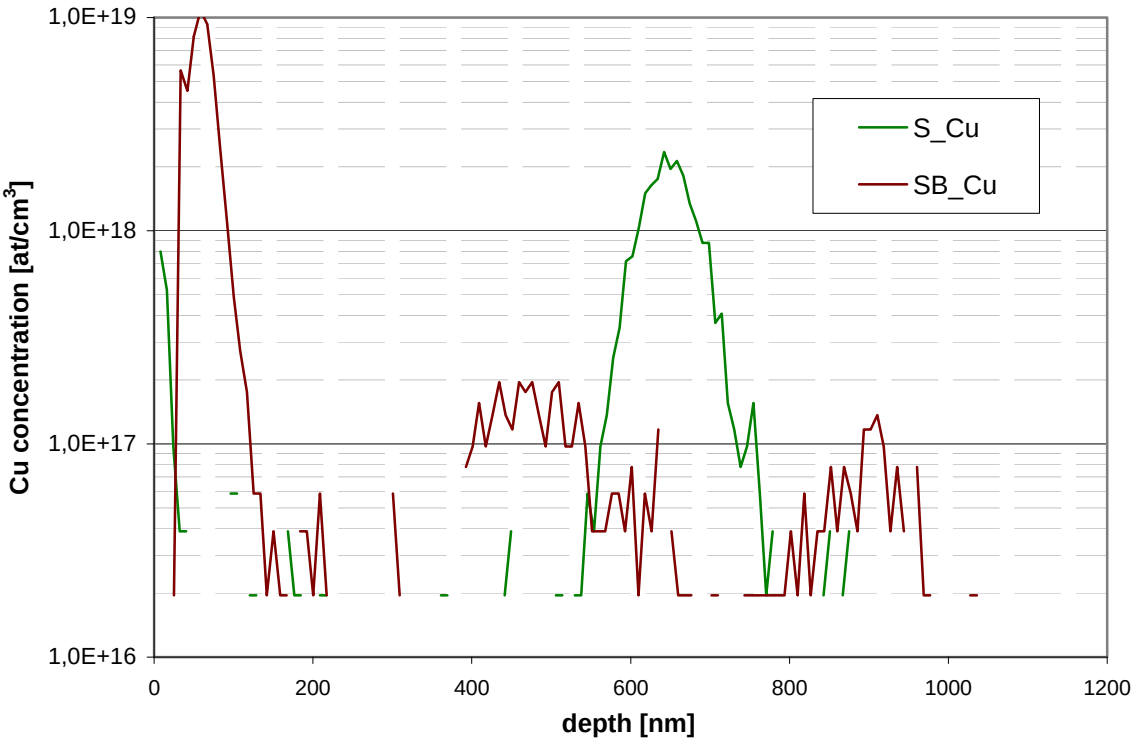

Figure 29: Quantified depth profiles of samples implanted by silicon ions

Sample S shows a very strong Cu peak for gettering in the R_p depth shifted to deeper regions of 640 nm, while the second sample implanted by Si^+ ions presents a Cu band that is moved to a somewhat smaller depth. For sample S no signs of an $R_p/2$ or a trans-R_p Cu gettering effect are evident, whereas sample SB shows a definite gettering band in regions deeper than the projected ion range but featuring less concentrations of copper therein, than accumulated in the R_p range.

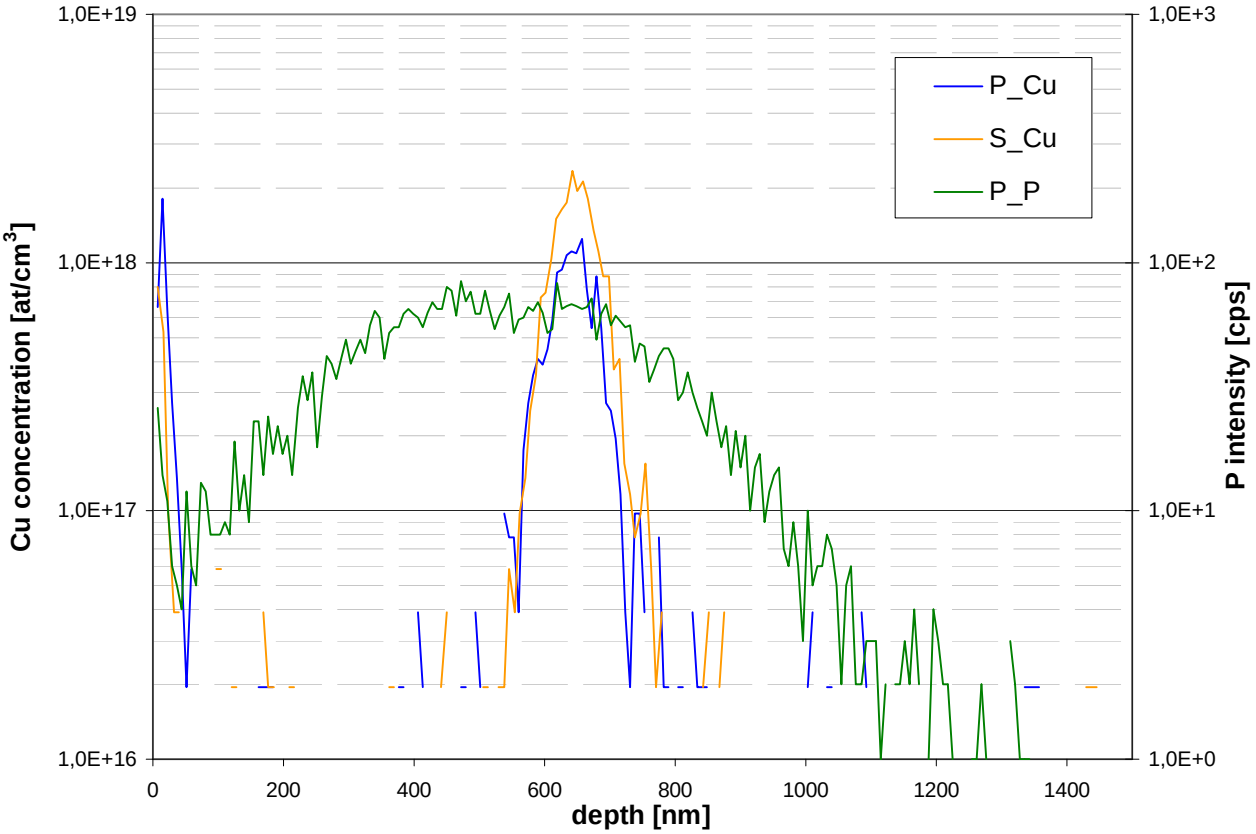

Figure 30: Comparison of samples implanted by phosphorus and silicon ions at 450 keV

The projected ion range for P+ and Si+ ions are slightly below 600 nm while both samples show a strong peak for Cu gettering in the R_p region that is apparently somewhat shifted to a greater depth. For both samples S, and P no additional gettering effects in the $R_p/2$ or trans-R_p range could be observed.

5.2 Na Diffusion in Silicon

Preliminary examinations of pure water showed difficulties to obtain a droplet size smaller than the analysis window of the TOF-SIMS instrument. Droplet sizes barely fitting a raster of 500x500 µm needed for SIMS investigation were achieved releasing the lowest possible amount of solution onto the surface. Sodium intensities will not be exactly comparable as the volume of the droplets varies due to inaccuracies of manual control of the application onto the surface.

Droplets:

volume [µl]	**average diameter Ø [µm]**
0,5	**1474**
0,3	**1222**
0,2	**1061**
0,1	**809**
0,08	**746**
0,04	**606**
0,02	**431**

Table 3: Average size of droplets on the silicon wafer surface as produced with the Hamilton syringe

Droplets of these two solutions act differently when applied onto the silicon wafer. Droplets of sodium carbonate were well wetting the silicon surface evenly. As these desiccated, sodium carbonate residues showed regular circles with crystal-like structures under the microscope throughout the experiments. On the other side, droplets of sodium acetate solutions grew into rough uneven structures of various forms. Also their hygroscopic behaviour when exposed to exhaled air could be observed under the microscope as they altered shape and structure.

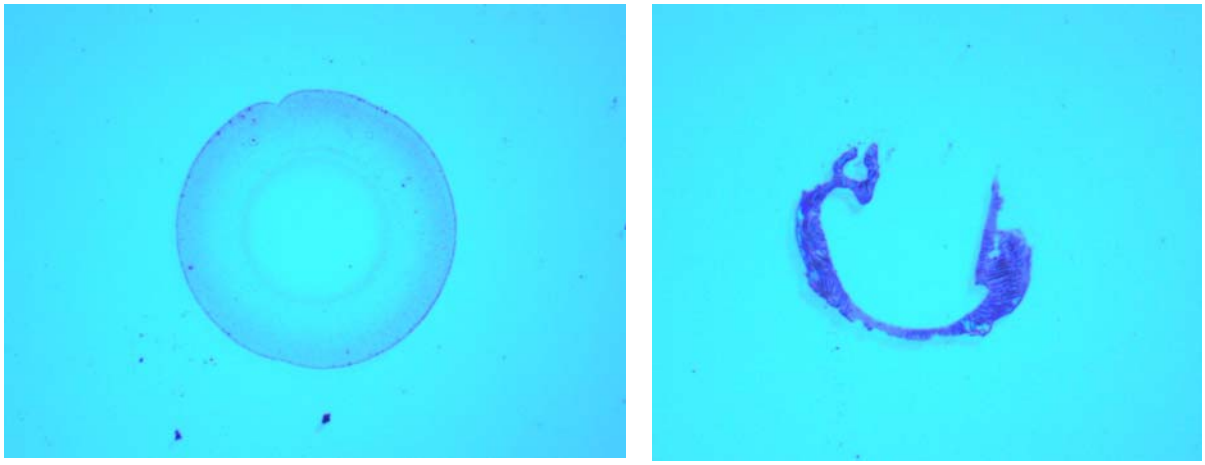

Figure 31: **Residues of droplets of sodium carbonate solution (left) and sodium acetate solution (right), respectively**

After applying the solutions onto the silicon samples different thermal treatments were carried out by means of furnace annealing to investigate thermal sodium surface diffusion. The furnace used for annealing procedures is also operated by other members of the research group. Thus, contaminations including sodium could to a certain amount derive from heat treatments in the furnace.

Sodium distributions for both carbonate and acetate solutions, respectively in general show similar behaviour. In principle, highest sodium concentrations were observed for low temperature annealed samples. Silicon wafers at room temperature or annealed up to temperatures of 280°C and 450°C, respectively show a broad high intensity sodium band at the surface slowly decreasing as measurements explore greater depths. A big leap can be found as annealing temperatures increase to 600°C and 750°C, respectively as a broad sodium peak is visible at the surface region, rapidly descending to relatively low intensities.

The temperature dependence of the diffusion coefficient of sodium diffusion in silicon bulk material was investigated by *Korol et al*. [28, 29], and *Belikova et al* [30]. They suggest the diffusion prefactor D_0 to be of a value of $1{,}5*10^{-6}$ and $1{,}0*10^{-6}$ [m^2/s], respectively concluding an activation energy of 122 [kJ/mol].

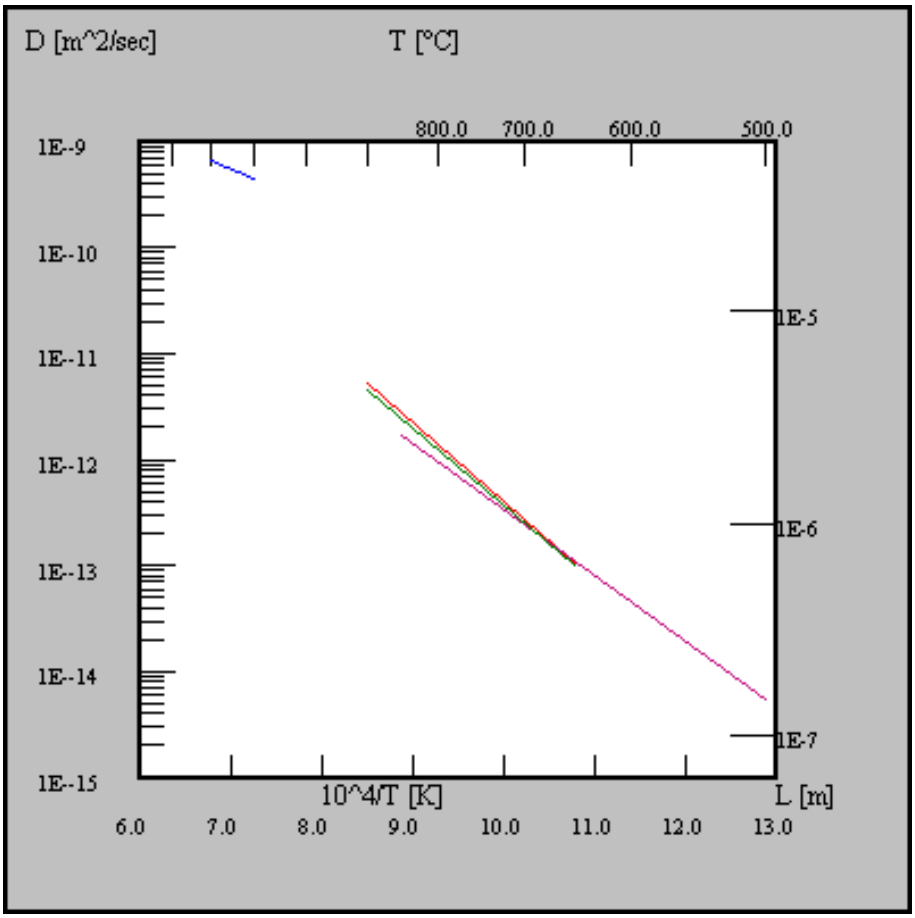

Figure 32: Diffusion coefficients for sodium in silicon bulk material

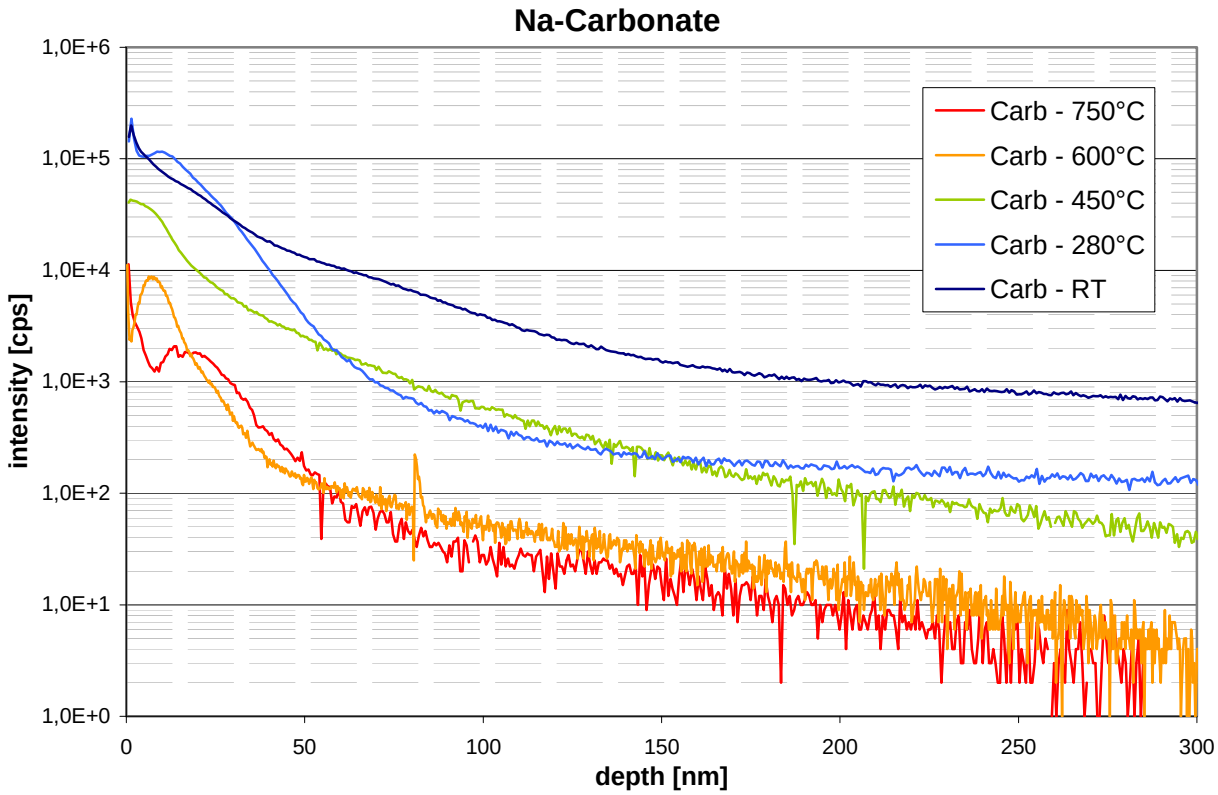

Figure 33: Depth profiles of sodium after applying sodium carbonate solution

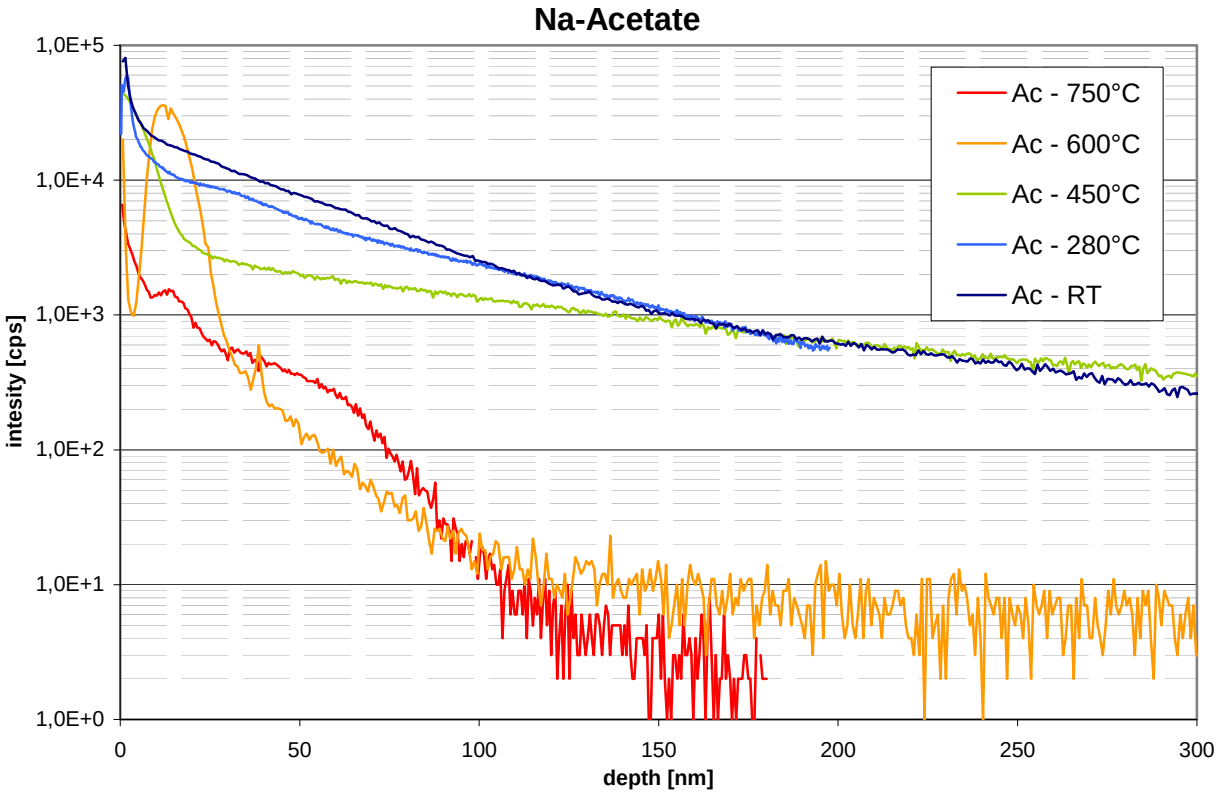

Figure 34: Depth profiles of sodium after applying sodium acetate solution

Sodium intensities for 600°C annealed samples show a distinct peak for sodium accumulations slightly below the surface. For the acetate contaminated sample this peak is pronounced much stronger. Whereas for even higher annealing temperatures of 750°C the peak strongly decreases and the sodium band broadens as it is shifted to deeper regions.

For sodium carbonate solutions somewhat sharper peaks for high temperature annealed samples are revealed. Sodium acetate samples show a much more broadened sodium band in this region.

Since the desiccated droplets are structures that are elevated above the surficial area of the sample, surface roughness induced peak broadening occurs. Areas around the protruding structure of the dried droplet are sputtered away, whereas the concentrations in the residue structure appear until the entire residue is removed and the silicon wafer bulk is reached. In Fig. 35 typical SIMS measurement craters after applying sodium carbonate (left) and sodium acetate (right) solution droplets onto the silicon wafer surface are shown. The broad dispersion of carbonate droplets and the mountainous structure of acetate droplet residues is clearly visible.

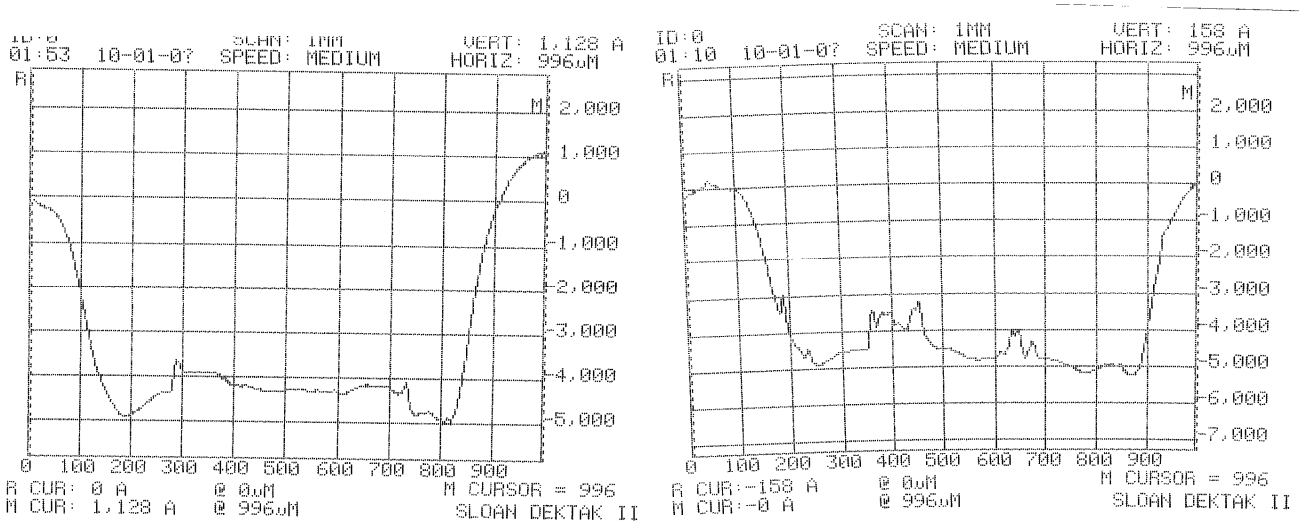

Figure 35: **Crater depth profiles measured after SIMS measurements by the Dektak II stylus profilometer**

The more regular structures of the sodium carbonate residues are mostly flat contrary to remainings of acetate droplets. These are elevated higher and are much more uneven and rough. Therefore, for sodium acetate sodium intensities are shifted to deeper regions.

As the samples are annealed in the furnace, the silicon wafer establishes oxide layers on the sample surface. Since the samples were all sputtered using the oxygen ion sputter gun only relative intensities of oxygen including sputtered atoms in the uppermost surface are shown. Although, it can be clearly seen, that at room temperature no extra oxygen is observed in the surface layers. For low temperature treated samples only little increase in additional oxygen intensities is visible, whereas the highest oxygen concentrations are definitely observed for samples annealed at the highest investigated temperatures. This effect can lead to deviations of measured sodium concentrations in regions close to the surface.

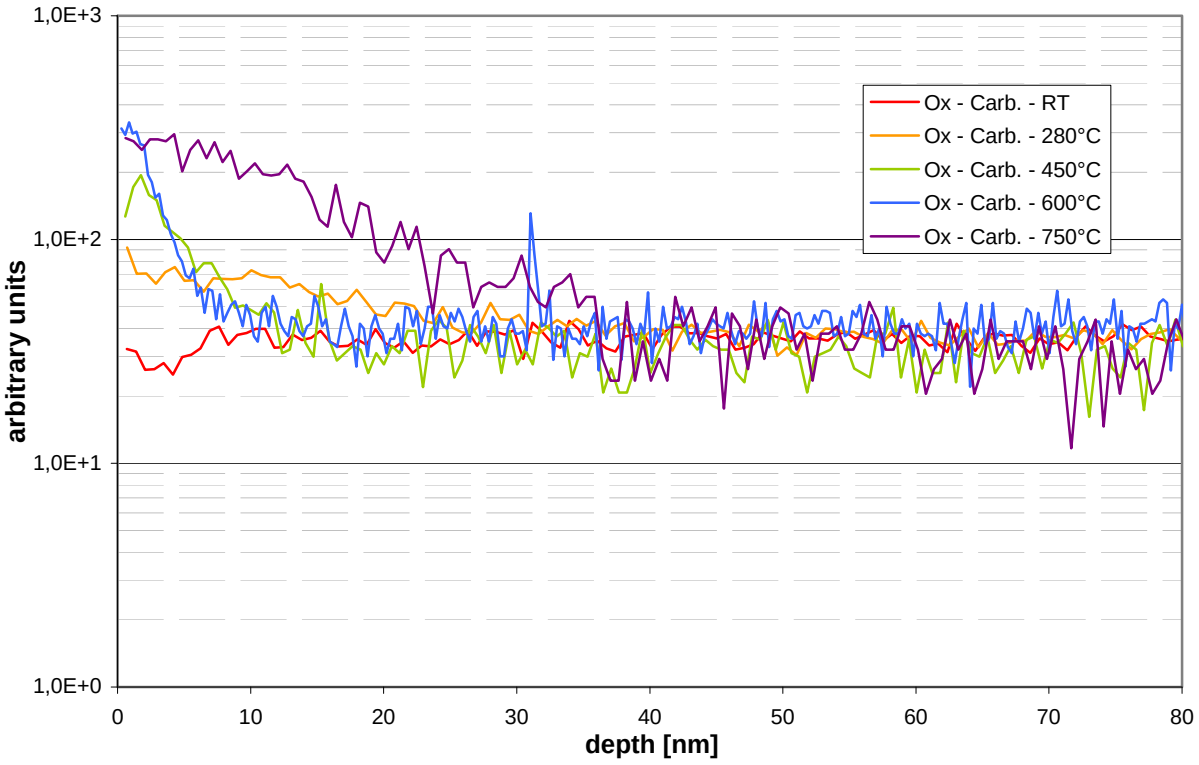

Figure 36: Oxygen distribution in top layers of sodium carbonate contaminated samples

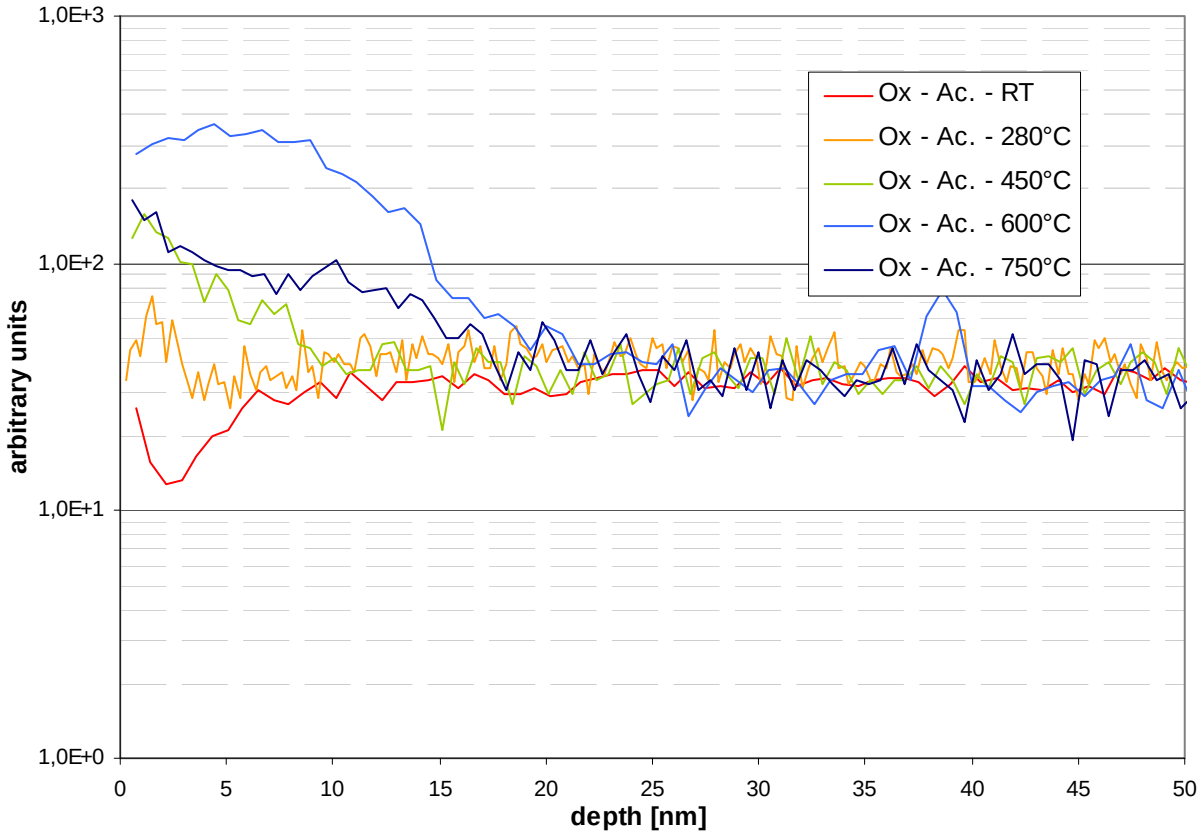

Figure 37: Oxygen distribution in top layers of sodium acetate contaminated samples

6 Conclusion

6.1 Cu Gettering

The implantation of oxygen ions into n-type silicon shows for both annealing times of 30, and 240 min, respectively the same copper gettering behaviour. Increasing times for thermal treatment does not lead to any changes in Cu gettering. Equal amounts of copper are accumulated in the R_p region, whereas no signs of $R_p/2$ or trans-R_p gettering effects appear. Oxygen gettering also shows similar shape for both annealing times.

In the boron doped sample for short annealing times strong oxygen gettering is observed, which entirely disappears after a substantially extended annealing period. Copper gettering is detected in the R_p and the $R_p/2$ range but distinct peaks are difficult to distinguish. A discrete peak appears in the trans-R_p range for both boron doped samples, slightly more pronounced and shifted to deeper regions when heat treatment is extended.

Oxygen and copper gettering effects are competitive at the dislocations and cavities in the R_p and $R_p/2$ region, respectively. As for in oxygen ion implanted samples of boron doped silicon all three oxygen gettering bands disappear for longer annealing times, while copper accumulations tend to increase somewhat over the entire gettering range, this different behaviour reflects a different trapping mechanism.

Supposedly the phosphorus ion implantation into silicon wafers was done by different energies of 200 and 450 keV, respectively as implied by sample descriptions provided to us. Nevertheless, after our investigations it was concluded that for both samples equivalent energies of 450 keV must have been used. Soon after investigations, this was confirmed by our partner Dr. Kögler.

Both P^+ ion implanted samples show a broad phosphorus band at the expected implantation range, being slightly broader for n-type silicon. The copper gettering again shows a broad distribution including an evident trans-R_p peak for the boron doped sample, whereas only a strong peak at R_p for n-type silicon could be observed. Similar gettering occurrences were observed for Si^+ ion implanted silicon wafers although, differences in intensities and depths can be noticed. Stronger R_p gettering of copper in n-type silicon is observed for Si^+ ion implantation. Both, P^+ and even Si^+ implanted boron doped silicon wafers show noticeable copper accumulations in the trans-R_p range. While a greater peak in this region is observed for the P^+ ion implanted sample, does the Si^+ ion implantation lead to a shift of the trans-R_p gettering band to greater depths.

All highly boron doped silicon wafers present a broad copper gettering band with hardly distinguishable peaks for $R_p/2$ and R_p regions, whereas all of them show a precise peak in the trans-R_p region.

The n-type silicon samples all reveal only gettering in the R_p region with equal concentrations except for P^+ ion implantation, which leads to a somewhat smaller copper gettering peak.

In general, similar expected results were found for oxygen, phosphorus, and silicon ion implantation into n-type silicon but tremendous disagreements occur for silicon wafers that were doped by

exceptionally high concentrations of boron atoms for identical sample production parameters.

These TOF-SIMS investigations of copper as metal trace element in silicon wafers have shown comparable results to previous measurements done using the former SIMS instrument of this research group, although detection limits for the ION-TOF^5 instrument are at higher concentrations. Copper quantification was done by the use of standards with well known copper concentrations.

6.2 Na Surface Diffusion

Our preliminary studies for sodium surface diffusion into silicon of two different contamination molecules shows strong dependence on temperature. A tremendous leap is observed for samples annealed at temperatures at 600°C and higher as sodium intensities strongly decrease. Activation energy for sodium surface diffusion into silicon may be reached at temperatures above 600°C as at these temperatures sodium vanishes into the bulk and intensities dramatically decrease at the surface. For low temperature measurements remarkably the sodium concentrations stays high even in a few hundreds nm depth. To be able to make accurate statements and understand sodium surface diffusion effects in detail further investigations are essential.

Intensities for sodium may include uncertainties due to handling of the droplets and the roughness of the remaining residues. During furnace annealing, silicon oxide layers at surface regions increase. These oxide layers at the surface can also have an effect on surface diffusion as they increase the activation barrier for diffusion from the surface into the bulk.

7 References

[1] R A Yankov, N Hatzopoulos, W Skorupa, A B Danilin; Nucl. Instrum. Meth. Phys. Res. B (1996) 120, 60-63

[2] J Czochralski; Z. Phys. Chem. (1918), 92, 219-221

[3] Y Nishi, R Doering; Handbook of Semiconductor Manufacturing Technology, McGraw-Hill Professional, (2005) 70-74

[4] US Patent 2787564, Bell Laboratories, (1954)

[5] R Kögler, M Posselt, R A Yankov, J R Kaschny, W Skorupa, A B Danilin; Mat. Res. Soc. Symp. Proc. (1997) Vol. 469, 463

[6] R A Brown, O Kononchuk, G A Rozgonyi, S Koveshnikov, A P Knights, P J Simpson, F Gonzalez; Jour. Appl. Phys. (1998) 84, 2459

[7] V C Venezia, D J Eaglesham, T E Haynes, A Agarwar, D C Jacobson, H-J Gossmann, F H Baumann, Appl Phys. Lett. (1998) 73, 2980

[8] R Kögler, R A Yankov, J R Kaschny, M Posselt, A B Danilin, W Skorupa, Nucl. Instrum. Meth. Phys. Res. B (1998) 142, 493

[9] R Kögler,A Peeva, J Kaschny, W Skorupa, H Hutter, Nucl. Instrum. Meth. Phys. Res. B (2002) 186, 298-302

[10] Y M Guergiev, R Kögler, A Peeva, D Pankin, R A Yankov, W Skorupa, J. Vac. (2001) 62, 309-313

[11] Y M Guergiev, R Kögler, A Peeva, D Pankin, R A Yankov, W Skorupa, Appl. Phys. Lett. (1999) 75, 22

[12] Y M Guergiev, R Kögler, A Peeva, D Pankin, R A Yankov, W Skorupa, J. Appl. Phys. (2000) 88, 11, 6934

[13] R F K Herzog , F P Viehböck, Phys. Rev. (1949) 76, 855-6

[14] T Grehl, Dissertation (2003) 12-14

[15] M L Yu, Phys. Rev. Lett. (1978) 40, 9, 574

[16] A Villegas, Y Kudriavtsev, A Godines, R Asomoza, Appl. Surf. Sc. (2003) 203-204, 94-97

[17] M L Yu, N D Lang, Nucl. Instrum. Methods B (1986) 14, 403

[18] R Kersting, Dissertation (2002) 10-11

[19] L W Swanson, Nucl. Instr. Meth. in Phys. Research (1983) 218, 347

[20] ION-TOF TOF-SIMS Help file

[21] S G Alikhanov, Sov. Phys. JETP (1957) 4, 452

[22] J F Ziegler, J P Biersack, U Littmark, The stopping and range of ions in solids, Pergamon Press, (1985)

[23] S Puchner, Diplomarbeit (2007) 8-9

[24] K Gammer, Dissertation (2003) 33-34

[25] R Kögler, A Peeva, J Kaschny, A Lebedev, M Posselt, W Skorupa, G Özelt, H Hutter, M Behar, J. Appl. Phys. (2003) 94, 6, 3834

[26] D Krecar, M Fuchs, R Kögler, H Hutter, Anal. Bioanal. Chem. (2005) 381, 1526-1531

[27] D Krecar, M Fuchs, R Kögler, H Hutter, Appl. Surf. Sc. (2005) 252 278-281

[28] V M Korol, A V Zastavnyi, M N Belikova, Fiz. i Tek. Polupr. (1975), 9(6), 1222

[29] V M Korol, Phys. Stat. Solidi A (1988) 110, 9-34

[30] M N Belikova, A V Zastavnyi, V M Korol, Scientific Res. Phy. Inst. (1976) 10, 319-20